A Combined SNIFTIRS and XANES Study of Electrically Polarized Copper Electrodes in DMSO and DMF Solutions of Cyanate (NCO^-), Thiocyanate (NCS^-) and Selenocyanate ($NCSe^-$) Ions

L. K. H. K. Alwis,[a] Michael R. Mucalo,[a,z] Bridget Ingham,[b,c] and Peter Kappen[d]

[a]*Chemistry, School of Science, Faculty of Science and Engineering, The University of Waikato, Hamilton 3240, New Zealand*
[b]*Callaghan Innovation, Lower Hutt 5040, New Zealand*
[c]*The MacDiarmid Institute for Advanced Materials and Nanotechnology, Wellington 6440, New Zealand*
[d]*Australian Synchrotron, Clayton VIC 3168, Australia*

A SNIFTIRS (subtractively normalized interfacial Fourier transform infrared spectroscopy) and X-ray absorption spectroscopy (XAS) study of electrically polarized copper electrodes in six polar aprotic solvent-based systems is presented. In the systems investigated, i.e. dimethyl formamide (DMF) and dimethyl sulfoxide (DMSO) solutions containing pseudohalide species of cyanate (NCO^-), thiocyanate (NCS^-) and selenocyanate ($NCSe^-$) codissolved with tetrabutylammonium perchlorate (TBAP), Cu was found to dissolve over a wide range of potentials to produce the corresponding Cu(I) pseudohalide and/or Cu(II) pseudohalide complex ion species. Insoluble deposited films were also observed at higher anodic applied potentials, thought to be CuSCN in the Cu/NCS^-/DMSO or DMF systems, and solid $K(SeCN)_3$ in the Cu/$NCSe^-$/DMSO or DMF systems respectively. The presence of the Cu(II) and/or Cu(I) oxidation states in complexes formed by polarization in Cu/pseudohalide ion systems in DMSO was clearly proven using XAS of cell solutions sampled after SNIFTIRS/electrical polarization experiments. In addition, Fourier transform infrared (FTIR) and X-ray absorption near edge spectroscopy (XANES) data obtained from model solutions prepared from mixing Cu(I) and/or Cu(II) salts with the respective pseudohalide ions in DMF and DMSO confirmed the speciation observed in the electrochemical experiments.

 [DOI: 10.1149/2.0321507jes]

Manuscript submitted December 10, 2014; revised manuscript received February 26, 2015. Published April 2, 2015.

A wide variety of organic solvents are used in technological processes,[1] for example, electrodepositing of copper from non-aqueous solutions.[2] In battery applications, the use of organic solvents like acetonitrile, for instance, allows use of the battery at low ambient temperatures.[3] However, extensive electrochemical characterization of metal electrode action (e.g. dissolution and electrodeposition) in non-aqueous (organic) media has been lacking. For instance, even though copper in DMF is widely used in industry, few electrochemical studies of copper dissolution/reduction in DMF have been reported.[4–7] The same may be said for electrodissolution studies in DMSO. Thiocyanate ion has often been used in copper electrochemistry, as it can mimic the behavior of halide ions like chloride,[8] which disrupt the passivation layer of oxide coatings formed on copper, and consequently increase the corrosion rate. The electrochemistry of metal electrode/pseudohalide systems has previously been studied by Bowmaker et al.[9,10] and Kilmartin et al.,[8,11] who looked at thiocyanate interaction with copper anodes and platinum electrodes. In addition, Bron and Holze have also reported in situ IR work for thiocyanate and cyanate interactions with gold and copper electrodes in aqueous electrolytes.[12] In situ IR spectroelectrochemistry can provide detailed information on electrochemical processes.[13–22] It is also valuable for characterizing the molecular species generated, especially in conjunction with conventional electrochemical techniques such as cyclic voltammetry, which is unable to identify discrete molecular compounds. Thiocyanate (and other pseudohalide ions) can be detected easily using IR spectroscopy, because the signal from the –CN moiety occurs in a region of the spectrum where few other fundamental vibrations are detected (2500–1800 cm^{-1}), thus allowing any speciation that occurs as a result of electrochemical processes to be followed. Monitoring the IR frequencies of the pseudohalide ion allows facile detection of species that form from electrical polarization of the metal in the non-aqueous electrolyte containing pseudohalide ion. Earlier work published by our group focused on electrogenerated products derived mostly from *anodic* polarization of nickel and gold electrodes in the presence of pseudohalide ions dissolved in DMSO and DMF solutions.[13,23,24] This work found that the predominant speciation of nickel in this system was as Ni^{2+} complex ions coordinated to pseudohalide ion and solvent molecules (i.e. DMF, DMSO). This investigation was supported by comparison with model solutions containing Ni^{2+} and pseudohalide ions dissolved in solvent. These gave IR spectra consistent with those obtained when the nickel electrode was anodically polarized in solution in the presence of each respective pseudohalide ion. A difference in speciation was noted for Ni anodically polarized in the presence of cyanate-containing electrolytes, as opposed to thiocyanate or selenocyanate-containing electrolytes. The species detected in the case of cyanate-containing electrolytes was the tetrahedral $[Ni(NCO)_4]^{2-}$ ion, which gave a characteristic blue coloration in DMSO or DMF solutions. In the case of anodic polarization of Ni in the presence of NCS^-- and $NCSe^-$-containing electrolytes, an octahedrally coordinated ion of the formula $[Ni(solvent)_5(NCX)]^+$ was posited as the species in solution. This was confirmed in later published X-ray absorption spectroscopy (XAS) results.[24] Similar in situ IR spectroscopy work from our laboratory on the Au/pseudohalide systems in DMF and DMSO showed the predominance of the Au(I) oxidation state in the electrochemically generated products detected.[23] The aim of the present study is hence to better understand the polarization behavior and speciation of copper electrodes in non-aqueous, polar aprotic solvents, i.e. DMSO or DMF-containing solutions of pseudohalide ions (NCO^-, NCS^- and $NCSe^-$) through investigation of electrogenerated products in solution. These products may be dissolved solution or gaseous species and electrodeposited solids on the electrodes. We have used a similar suite of techniques as in the earlier studies of Ni electrodes anodically polarized in pseudohalide-containing DMSO or DMF electrolytes,[13,24] namely in situ IR spectroelectrochemical methods combined with synchrotron X-ray absorption near edge spectroscopy (XANES). A study was undertaken both of cell solutions containing electrogenerated products, and model solutions prepared that mimic these species independently of the electrolysis process. The results serve to provide a greater fundamental understanding of the electro-dissolved species

[z]E-mail: mucalo@waikato.ac.nz

and solid electrodeposition products that form from the interaction of copper and pseudohalide ions in non-aqueous solutions under various conditions, such as those found during electrochemical processing (e.g. electrolysis) or corrosion.

Experimental

Reagents and solutions.— DMSO sourced from either Scharlau or Aldrich (99.9%) was used without further purification for all experiments described. DMF was sourced from Ajax Finechem Pty. Purities of solvents were as reported in reference.[13] The pseudohalide salts used in the experiments, i.e. potassium cyanate (KOCN, >96%), sodium and potassium thiocyanate (NaSCN, KSCN, >99%), and potassium selenocyanate (KSeCN, >97%), as well as tetrabutylammonium perchlorate (>98%) and XAS standards (Cu_2O and CuO powders, Cu foil), were obtained either from Aldrich Chemical Co, Ltd. or BDH Chemicals and were also used as received. Cu(I) and Cu(II) salts were used to prepare model solutions in DMSO and DMF. Cupric chloride ($CuCl_2.2H_2O$, Anal-R grade BDH chemicals) containing waters of crystallization was partially dehydrated in an oven at 50°C for 2–3 hours. This led to the originally blue salt turning a brown color after heating. Not all water was removed as confirmed by IR spectroscopic analysis; however this was not believed to greatly affect the results. The model solutions involving $CuCl_2$ were made by mixing partially dehydrated $CuCl_2$ and pseudohalide salts in various $CuCl_2$:pseudohalide salt mole ratios (from 1:1 to 1:8 depending on the pseudohalide salt and solvent used) to verify species detected in the electrochemical experiments. Another set of model solutions for IR spectroscopy experiments was made by mixing CuI (Ajax Chemicals Ltd. Australia) and pseudohalide salts in mole ratios (CuI : pseudohalide salt) of 1:1, 1:2 and 1:4 in DMSO but only 1:1 and 1:2 in DMF (due to solubility issues of the pseudohalide salt in DMF).

Spectroelectrochemical cell and electrode cell design.— The working electrode was a flat, circular polycrystalline piece of copper (Aldrich, 99.98% purity) 7 mm in diameter. The construction of this electrode and the thin layer IR spectroelectrochemical cell employed in this study are described previously,[13] with the thin layer cell (having a layer thickness of ca. 1.31 μm) being placed on top of a fixed angle (30°) Spectra Tech FT-30 specular reflectance accessory. Before each run, the Cu foil electrode was polished to a mirror finish with an aqueous alumina powder paste and then rinsed in distilled water (with the aid of an ultrasonic bath) prior to drying in air which was assumed to have removed most of any pre-existing oxide film.

IR spectroelectrochemistry.— Cyclic voltammetry (CV) was initially performed on all electrochemical systems that were studied by SNIFTIRS (subtractively normalized interfacial Fourier transform infrared spectroscopy) using an EDAQ computer-interfaced potentiostat system, with an AgCl/Ag reference electrode and Pt counter electrode, controlled by Echem software as described previously.[13] A single cycle from −800 mV to +2000 mV(AgCl/Ag) was acquired as the initial CV characterization. As described in earlier work,[13,18] subtractively normalized interfacial Fourier transform infrared spectra (SNIFTIRS) were obtained with a dry N_2-purged Biorad FTS-40 FTIR spectrometer using a liquid N_2-cooled InSb detector. The SNIFTIRS spectra were acquired by recording a background spectrum of the thin-layer cell at an initial background potential. In the case of the Cu/NCO^- electrochemical systems, the background spectrum was recorded at −1500 mV(AgCl/Ag) whereas with the Cu/NCS^- and Cu/$NCSe^-$ electrochemical systems, the background spectra were recorded at −900 mV(AgCl/Ag). The difference is due to the more electroactive nature of the Cu/NCO^- electrochemical systems at cathodic applied potentials relative to those systems containing NCS^- and $NCSe^-$ ions. IR spectra were then recorded at potentials more anodic than the chosen background potential and were ratioed against the relevant background spectrum. SNIFTIRS runs of each system were repeated in triplicate with a fresh, previously unused Cu electrode for each run. Electrochemical data in the form of current/potential curves were also collected during the SNIFTIRS experiments. The average current used at the copper electrode at each applied potential was calculated, since the cell current observed during the SNIFTIRS experiments changed slightly during acquisition of each spectrum. This value was calculated by averaging the current noted at the *beginning* of the IR data acquisition conducted for that applied potential value, and that noted at the *conclusion* of the spectral acquisition. The current tended to be higher at the beginning of an acquisition and decreased during the acquisition (see Table S1 for the raw current values for the beginning and end of each SNIFTIRS experiment). These data are presented as plots of average current vs. applied potential and have been distinguished in this study from the CV data by referring to them as "current/potential curves" of the Cu/pseudohalide electrochemical systems.

IR transmission spectra of the model solutions and other confirmatory solution preparation experiments were acquired as thin layers in conventional Press-Lok cells on a Perkin-Elmer Spotlight 200 FTIR instrument, as previously reported.[13]

XANES.— XANES measurements were performed on the XAS beamline at the Australian Synchrotron (Melbourne, Australia). Liquid samples were mounted in a custom made Perspex cell as used previously[24] which was fabricated by affixing Kapton tape to both sides of a conventional solid pellet holder. The holder had a circular cavity of 1.3 cm diameter by 2 mm thickness. Liquid was then injected into this Kapton-sealed cavity (∼2.5 ml) via syringe. The liquid-filled cell was then quickly frozen by immersion in liquid nitrogen and the XANES measured in a helium cryostat at ∼5 K to avoid the formation of bubbles due to ionization of the liquid solution by the X-ray beam and to mitigate radiation induced reduction of Cu(II). Due to time constraints, only the Cu-DMSO-based solution systems were studied with XANES. The nominal beam size at the sample was 2 × 0.5 mm (horizontal x vertical). XANES spectra were recorded in fluorescence mode at the Cu K-edge (8979 eV) using a Canberra 100-element Ge detector. Solid standards (Cu foil, Cu_2O, CuO) were measured in transmission mode by mixing the powdered oxide samples with cellulose powder in a weight ratio of approximately 1:10 ($\mu_T d \approx 1.5$), followed by gentle grinding by hand with a mortar and pestle, before being pressed into a disc. A liquid Cu(II) standard solution was prepared as nominally 0.05 mol L^{-1} of the partially dried cupric chloride in neat DMSO solvent. Extended X-ray absorption fine structure (EXAFS) was also attempted but unlike the Ni-based samples,[24] the Cu-based solutions were found to be susceptible to beam damage over extended periods of time so these measurements did not yield usable data for EXAFS. XANES results were also subject to beam damage during acquisition but were nevertheless found to be of utility in the study. To assess the extent of beam damage, multiple XANES scans were collected and only the first scan was used for analysis. XANES data were background-subtracted and normalized using the AUTOBK[25] routine in Athena.[26]

The following materials were measured as standards:

CuO (Cu(II) powder standard),
Cu_2O (Cu(I) powder standard),
$CuCl_2$ dissolved in DMSO (Cu(II) liquid standard).

The following samples were measured:

$CuCl_2$/KOCN dissolved in DMSO solvent (with mole ratios of Cu^{2+}:NCO^- of 1:1, 1:2, and 1:4 (model solutions) and cell solution from Cu electrode/KOCN electrochemical system after polarizing at +500 mV in the thin layer cell.
$CuCl_2$/KSCN dissolved in DMSO solvent (with mole ratios of Cu^{2+}:NCS^- of 1:1, 1:4 (model solutions) and the cell solution from the Cu electrode/KSCN electrochemical system after polarizing at +200 mV for 2–3 hours in the thin-layer cell.
$CuCl_2$/KSeCN dissolved in DMSO solvent (with mole ratios of Cu^{2+}:$NCSe^-$ of 1:1, 1:4 (model solutions) and 1 cell solution from the Cu electrode/KSeCN electrochemical system after polarizing at +400 mV for 2–3 hours in the thin-layer cell.

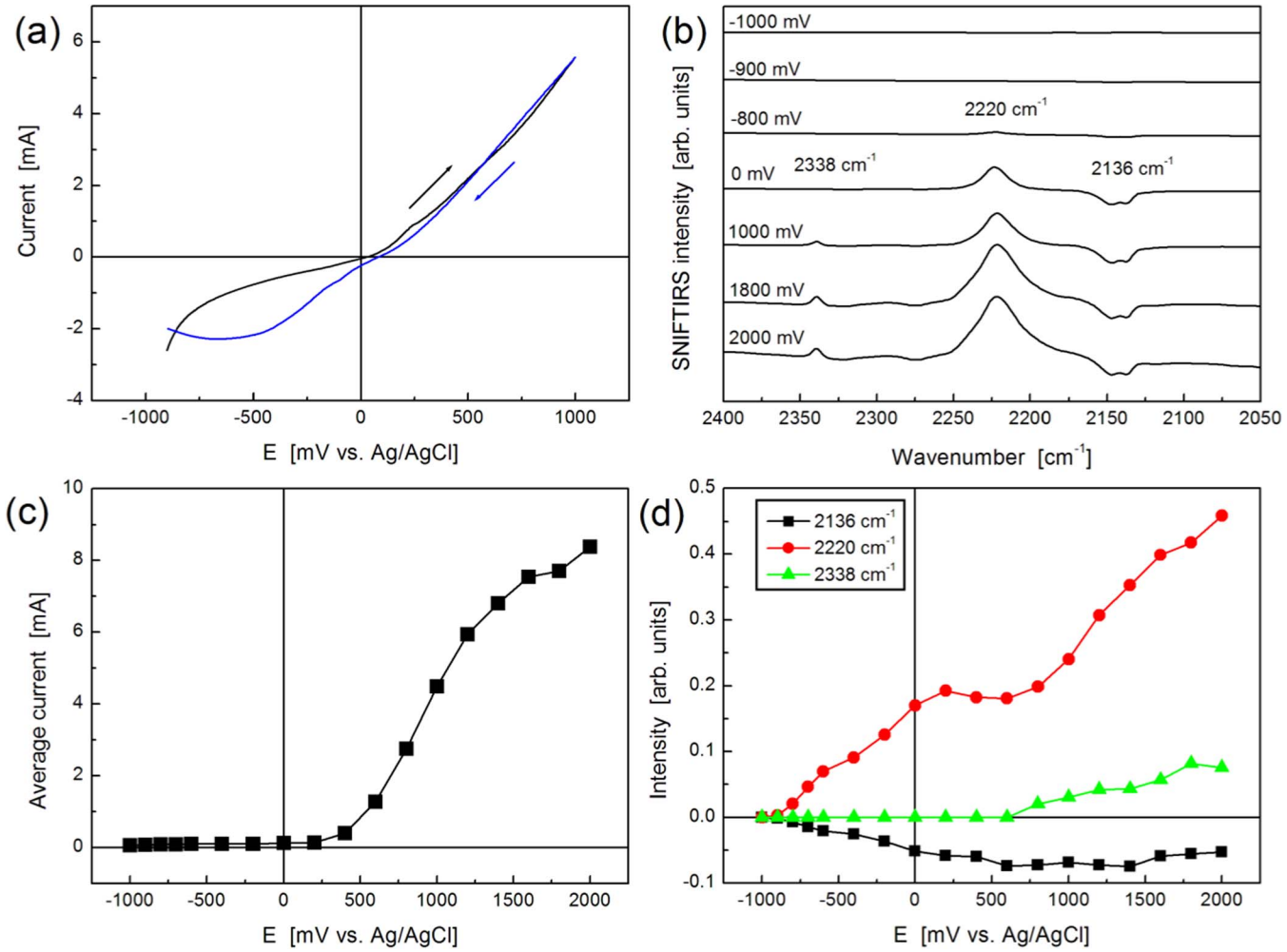

Figure 1. Combined electrochemical and SNIFTIRS-related data pertaining to the copper electrode system in DMF electrolyte containing 0.025 mol L^{-1} KOCN and 0.1 mol L^{-1} TBAP: (a) CV (sweep rate = 20 mV/s, arrows show the path actually traced upon conducting the potential sweep), (b) SNIFTIRS spectra of the copper electrode as a function of applied potential, (c) Current/potential data acquired of the copper electrode during SNIFTIRS experiments (current was averaged at the beginning and end of the acquisition period for each applied potential), and (d) Intensity changes of SNIFTIRS-detected peaks corresponding to the various molecular species generated in the thin layer from the copper electrode: free NCO^- (2136 cm^{-1}), $[Cu(I)(NCO)_2]^-$ (2220 cm^{-1}), CO_2-DMF (2338 cm^{-1}).

Results and Discussion

Cu/NCO⁻ systems.— Figure 1 and Figure 2 show the CV, SNIFTIRS spectra, current/potential plots and IR intensity data for the Cu/NCO^- electrochemical systems in DMF and DMSO respectively.

CV investigations of the Cu/TBAP/NCO⁻/DMF and DMSO systems.— The cyclic voltammogram (CV) of the copper electrode in DMF and DMSO solvents containing 0.025 mol L^{-1} KOCN recorded under the thin-layer condition, with 0.1 mol L^{-1} TBAP as an inert supporting electrolyte, reproducibly showed the curves illustrated in Figure 1a and 2a.

The voltage was adjusted between −800 mV(AgCl/Ag) and +1000 mV(AgCl/Ag) for the Cu/DMF/NCO^- system. The CVs for the Cu/NCO^- electrochemical systems in both DMF and DMSO showed a largely featureless region from −800 mV(AgCl/Ag) to 0 mV(AgCl/Ag). Above 0 mV(AgCl/Ag), an increase in (positive) current was observed which was interpreted as being due to the oxidation of Cu and other concurrent processes such as solvent oxidation, and pseudohalide ion oxidation. When the voltage was reversed at +2000 mV, no apparent reduction feature was observed in the CVs of either system, which indicates that the oxidation of copper was irreversible and that the species were released from the electrode surface into the solution.

IR spectra of Cu/TBAP/NCO⁻/DMF and DMSO.—Figure 1b and 2b present the series of IR spectroelectrochemical spectra (SNIFTIRS) that were recorded of the copper electrode using 0.025 mol L^{-1} KOCN and 0.1 mol L^{-1} tetrabutylammonium perchlorate (TBAP) in DMF and DMSO respectively, relative to the potential at which the background spectrum was recorded i.e. −1500 mV (AgCl/Ag). Figure 1c and 2c present the current/potential data plots showing the average current measured at each applied potential in the thin layer cell during the SNIFTIRS experiment. Figure 1d and 2d show the plots of the intensity changes of SNIFTIRS peaks observed in the Cu/TBAP/NCO^-/DMF and DMSO systems as a function of applied potential. Table I gives the frequencies of the IR peaks observed for both Cu/NCO^- electrochemical systems studied.

The current/potential data plots for the Cu/NCO^- systems in DMSO and DMF have similar features, i.e. a "flatline" of low current at cathodic potentials and an increasing anodic current when the applied potential was raised above +500 mV(AgCl/Ag). Although the current in the cathodic polarization region was observed to be small in the current/potential plots, it is apparent from in situ IR spectra (see Figure 1b and 2b) that features due to oxidized Cu species were appearing in both the DMF and DMSO systems in that region of cathodic applied potential. Peaks were observed at frequencies of 2136, ca. 2220 cm^{-1}, and 2338 cm^{-1}. The peak observed at 2136 cm^{-1} in Figure 1b and 2b is attributed to free NCO^- ions in the electrolyte.[13]

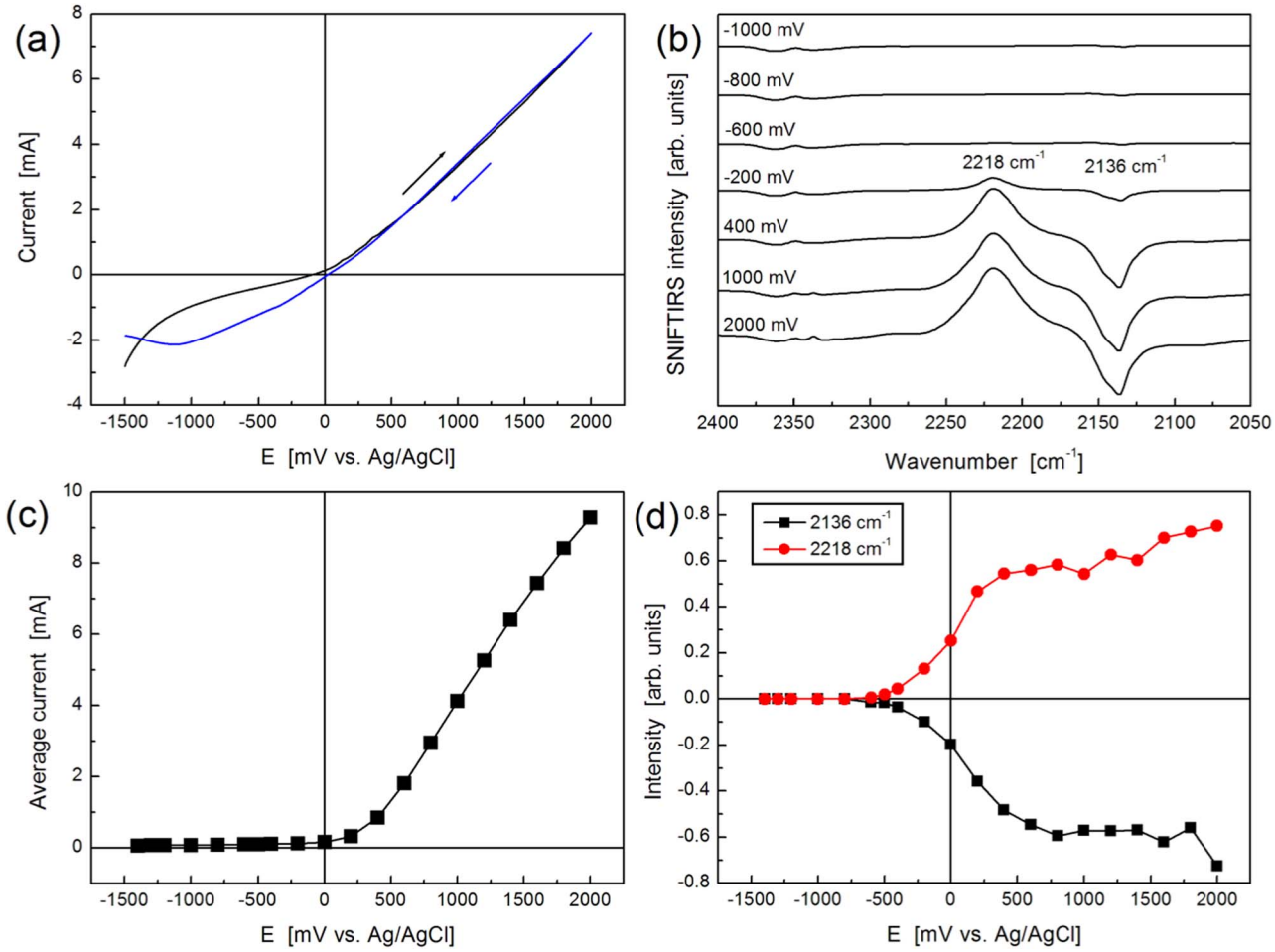

Figure 2. Combined electrochemical and SNIFTIRS-related data pertaining to the copper electrode system in DMSO electrolyte containing 0.025 mol L^{-1} KOCN and 0.1 mol L^{-1} TBAP: (a) CV (sweep rate = 20 mV/s, arrows show the path actually traced upon conducting the potential sweep), (b) SNIFTIRS spectra of the copper electrode as a function of applied potential, (c) Current/potential data acquired of the copper electrode during SNIFTIRS experiments (current was averaged at the beginning and end of the acquisition period for each applied potential), and (d) Intensity changes of SNIFTIRS-detected peaks corresponding to the various molecular species generated in the thin layer from the copper electrode: free NCO^- (2136 cm^{-1}), $[Cu(I)(NCO)_2]^-$ (2218 cm^{-1}).

This is normally observed as a negative-going peak in SNIFTIRS spectra, indicating that the amount of cyanate ion in the thin layer decreased as the applied potential was increased in the anodic direction.

The peak at 2338 cm^{-1} was observed in the Cu/NCO^- systems in DMF (and also in Ni/NCO^-/DMF or DMSO electrochemical systems)[13] at very positive applied potentials (>+1000 mV (AgCl/Ag)). This was attributed to electrogenerated, dissolved CO_2 in the DMF solvent,[13] and is formed from oxidation of dissolved cyanate, and in DMF systems from electro-oxidation of the solvent in the electrolyte medium.

The weak broad peak at 2220 cm^{-1} in Figure 1b and 2b began to emerge at potentials >−800 mV(AgCl/Ag) in DMF and

Table I. FTIR data from in situ IR spectroelectrochemical studies of Cu/NCX^- systems electrochemically polarized in 0.1 mol L^{-1} TBAP in DMSO or DMF solvents.

Electrolyte	ν(CN) of free NCX^- ion (X = O, S, Se,) cm^{-1}	ν(CN) of Cu^+/NCX^- (or Cu^{2+}/NCX^-)[a] complex ion or insoluble films of CuSCN or $K(SeCN)_3$ cm^{-1}	ν(CO) of CO_2 dissolved in solvent cm^{-1}	Color of cell solution after SNIFTIRS experiment
Cu/DMF/NCO^-	2136	2220	2338	light green
Cu/DMF/NCS^-	2055	2087, 2173[b]	2338	red
Cu/DMF/$NCSe^-$	2066	2087, 2140[c]	nd	gold yellow
Cu/DMSO/NCO^-	2136	2218	nd	light green
Cu/DMSO/NCS^-	2055	2087, 2171[b]	nd	red-yellow
Cu/DMSO/$NCSe^-$	2065	2089, 2138[c]	nd	gold yellow

nd = not detected.
[a]In electrolytes containing NCS^- and $NCSe^-$, the peak at 2087 cm^{-1} contains contributions from Cu^{2+} and Cu^+ complex ions coordinated to NCS^- or $NCSe^-$ ion.
[b]Solid CuSCN film.
[c]Solid $K(SeCN)_3$ film.

>−600 mV(AgCl/Ag) in DMSO. This peak is believed to be due to $[Cu(NCO)_2]^-$, a Cu(I) complex ion species. No specific IR data on this species exist in the literature, although spectroscopic data from Cu(II) cyanate species are described by several authors.[27,28] Forster and Goodgame[27] reported that nujol mull IR spectra of $(Et_4N)_2Cu(NCO)_4$ salts have ν(CN) stretching frequencies at 2183 cm^{-1} (strong) with a shoulder at 2247 cm^{-1}. Melendres et al.[28] observed a peak at 2234 cm^{-1} in the in situ IR spectra of a Cu electrode in 0.0001 M KOCN and 0.1 M $NaClO_4$ solution at −0.25 V (SCE), which they assigned to "a few monolayers of $Cu(OCN)_2$". A recent study by Ray et al.[29] reported crystallographic, electrochemical, and IR data on an end-on-end bridged Cu (I)-(II)/cyanate compound, $[Cu_2L_2Na(NCO)_2Cu]^n$ where L = N,N′ bis(2hydroxyacetophenone)propylenediimmine) which gave a ν(CN) stretch of 2228 cm^{-1} in IR spectra. This is the closest frequency to what is observed in the in situ IR spectra of the Cu/NCO^- system in the present study, so is the strongest literature evidence that exists showing that the 2220 cm^{-1} peak is a Cu(I) complex.

Other experimental evidence collected from the present study also suggested that this peak was due to a Cu(I) solution species. A sample of cell solution was extracted from the Cu/NCO^-/DMSO electrochemical system after the Cu electrode had been polarized at an initial potential of −800 mV(AgCl/Ag) for one hour. The IR transmission spectrum recorded of this cell solution showed two features at 2220 cm^{-1} and 2136 cm^{-1} (Figure S1). This constituted experimental proof that the 2220 cm^{-1} peak is due to a Cu(I) solution species released from the electrode surface.

Figure 1c and 1d and 2c and 2d summarize the current/potential data and intensity trends of species observed in the in situ IR spectra as a function of applied potential in the Cu/NCO^- electrochemical systems. Figure 1c and 2c show that the current increases from very small values in the cathodic applied potential region to a maximum of 9–10 mA in the anodic applied potential region. The electrochemistry in the system is at its most active after +500 mV(AgCl/Ag). As for the intensity trends, the negative intensity of the peak at 2136 cm^{-1} over all applied potentials studied reflects the consumption of the free cyanate ion species. The peak centered at 2220 cm^{-1} reflects this fact by showing a steady increase in intensity over all potentials tested but steps up in value in anodic applied potential regions. Interesting parallels may be drawn between this study and that of Bron and Holze's SNIFTIRS-type investigation[12] on cyanate and thiocyanate interaction with gold and copper electrodes in aqueous electrolytes. In their study, conducted in more dilute solutions of pseudohalide ion than the present work, adsorbed cyanate on copper electrodes was detected at −550 mV vs. SCE (saturated calomel electrode which is equivalent to −505 mV vs. AgCl/Ag) and was indicated by a potential-dependent broad band at 2203–2226 cm^{-1}. It was also remarked in the same study that cyanate adsorption on Cu occurred at more negative potentials relative to Au. As a comparison, an interesting feature of the presently studied Cu/NCO^- systems in DMF and DMSO was the "early" appearance of the peak due to the Cu(I) cyanate species in the SNIFTIRS spectra (see Figure 1b and 2b) at very negative applied potentials (i.e. >−800 mV(AgCl/Ag) in DMF and >−600 mV (AgCl/Ag in DMSO. This requires comment as it implies that the dissolution of the Cu electrode has occurred at these very cathodic applied potentials values which might seem unrealistic. There are several factors causing this. Firstly, the presence of complexing ligands like NCO^- can cause electro-oxidation of Cu at more negative values of the applied potential relative to systems where no complexing agents are present because of stabilization of the Cu(I) oxidation state. A second, and arguably the most important factor, may be the pre-existence of passivation layers on the Cu surface containing Cu^+ species despite the care in using pre-polished electrodes in SNIFTIRS experiments. Vojinovic et al.[4] reported that electrochemical deposition *and* dissolution of Cu in potassium perchlorate-containing DMF electrolytes compete with a passivation layer that is present. This passivation layer can form on the Cu electrode when it is immersed in DMF even under open circuit conditions. The layer was suggested by Vojinovic et al. to consist of adsorbed Cu^+ ions complexed with solvent molecules. The third factor which incidentally explains the prevalence of the Cu(I) oxidation state in these studies is the known stability of the Cu(I) state in polar aprotic solvents like DMSO, especially in the presence of stabilizing ligands like halides, as has been described in previous work by Ahrland.[30]

As a check on how CN^- (as opposed to NCO^- ion) interacts with a Cu electrode in DMSO media, SNIFTIRS data were acquired on a Cu/CN^- electrochemical system recorded under almost the same conditions (i.e. using TBAP as supporting electrolyte and dissolved KCN). The SNIFTIRS spectra from this experiment are presented in Figure S2 and feature a peak at 2085 cm^{-1} due to $[Cu(CN)_3]^{2-}$ which confirms, as in the Cu/NCO^- electrochemical systems, that Cu(I) species must pre-exist on the surface of the electrodes despite polishing. This affirms the reason for why Cu(I) complexes are observed in the SNIFTIRS spectra at the very negative potentials in the Cu/NCO^- electrochemical systems. It should also be added that unlike in Bron and Holze's study[12] no spectral evidence associated with (free) CN^- ion species produced by electroreduction of cyanate at the Cu electrode in DMF or DMSO electrolytes was observed in any of the SNIFTIRS studies of the Cu/NCO^- electrochemical systems.

Cu/NCO^-/DMF and DMSO model solutions.—To verify assignments of SNIFTIRS spectra-detected peaks in the Cu/NCO^- electrochemical systems, model solutions of the species of interest were prepared via a non-electrochemical method. Solutions were prepared for both Cu(I) and Cu(II) systems to determine the characteristic frequencies for cyanate complexes with each oxidation state of Cu. These model solutions were made by combining either solutions of cupric chloride or cuprous iodide with pseudohalide salts in various Cu: pseudohalide salt mole ratios (1:1 to 1:4 or 1:8 depending on the solvent used). Table II (for solutions of cupric chloride and pseudohalide salts) and Table III (for solutions of cuprous iodide and pseudohalide salts)

Table II. FTIR data from IR studies of DMF or DMSO model solutions of $CuCl_2$ and potassium (or sodium) pseudohalide ion salts prepared with different mole ratios.

Model solution studied and mole ratio of ($CuCl_2$): NCX^- prepared in DMF or DMSO (X = O, S, Se)	ν(CN) of free NCX^- ion (X = O, S, Se) cm^{-1}	ν(CN) of Cu^{2+}/NCX^- complex ion cm^{-1}	Observed color of model solution
DMF			
$CuCl_2$/ KOCN 1:1	nd	2194	green
$CuCl_2$/ KOCN 1:2	nd	2194	green
$CuCl_2$/ KOCN 1:4	2136	2196	blue green
$CuCl_2$/ NaSCN 1:1	2056	2090	blood red
$CuCl_2$/ NaSCN 1:2	2056	2088	blood red
$CuCl_2$/ NaSCN 1:4	2056	2084	blood red
$CuCl_2$/ KSeCN 1:1	nd	nd	gold yellow
$CuCl_2$/ KSeCN 1:2	2065	2092	orange brown
$CuCl_2$/ KSeCN 1:4	2065		orange brown
DMSO			
$CuCl_2$/ KOCN 1:1	nd	2202	green
$CuCl_2$/ KOCN 1:2	nd	2202	green
$CuCl_2$/ KOCN 1:4	2136	2196	blue
$CuCl_2$/ KOCN 1:8	2136	2196	blue
$CuCl_2$/ NaSCN 1:1	2055	2093	light red
$CuCl_2$/ NaSCN 1:2	2055	2093	red
$CuCl_2$/ NaSCN 1:4	2055	2090	blood red
$CuCl_2$/ NaSCN 1:8	2055	2089	blood red
$CuCl_2$/ KSeCN 1:1	2065	2096	gold yellow
$CuCl_2$/ KSeCN 1:2	2065	2096	gold yellow
$CuCl_2$/ KSeCN 1:4	2065	2096	orange brown
$CuCl_2$/ KSeCN 1:8	2065	2088	orange brown

nd = not detected.

Table III. FTIR data from IR studies of DMF or DMSO model solutions of CuI and potassium (or sodium) pseudohalide ion salts prepared with different mole ratios.

Model solution studied and mole ratio of (CuI): NCX^- prepared in DMF or DMSO (X = O, S, Se)	ν(CN) of free NCX^- ion (X = O, S, Se) cm^{-1}	ν(CN) of Cu^+/NCX^- complex ion cm^{-1}	Observed color of solution
DMF			
CuI/ KOCN 1:1	nd	2220	green
CuI/ KOCN 1:2	nd	2220	light green
CuI/ NaSCN 1:1	nd	2089	green
CuI/ NaSCN 1:2	2056 sh	2088	colorless
CuI/ KSeCN 1:1	2065 sh	2088	orange brown
CuI/ KSeCN 1:2	2065 sh	2088	colorless
DMSO			
CuI/ KOCN 1:1	nd	2220	green
CuI/ KOCN 1:2	nd	2220	light green
CuI/ KOCN 1:4	2136, 2147	2220	colorless
CuI/ NaSCN 1:1	nd	2088	green
CuI/ NaSCN 1:2	2055 sh	2088	yellow/green
CuI/ NaSCN 1:4	2055 sh	2088	colorless
CuI/ KSeCN 1:1	2065 sh	2088	red brown
CuI/ KSeCN 1:2	2065 sh	2088	yellow
CuI/ KSeCN 1:4	2065 sh	2088	colorless

nd = not detected; sh = shoulder

summarize all the IR spectroscopic data and include observations made of the model solution color.

Table II shows that when copper (II) chloride/potassium cyanate solutions in DMSO or DMF are prepared in Cu^{2+}: NCO^- mole ratios from 1:1 to 1:4 (DMF) or to 1:8 (DMSO), two peaks are detected in the ν(CN) stretching region at 2136 and 2194–2198 cm^{-1}. The peak at 2136 cm^{-1} is the vibrational peak of free cyanate ion in DMSO and DMF, as assigned earlier. It is also observed for the Cu^+:NCO^- 1:4 mole ratio solution in DMSO (Table III). This peak did not appear in the 1:1 and 1:2 mole ratio model solution spectra for either Cu(II) or Cu(I), but did appear in the 1:4 and 1:8 mole ratios, which indicates the total complexation of free NCO^- ions by copper ions in the model (cyanate-containing) solutions at mole ratios up to 1:2. Another feature observed for all model solution spectra for the Cu(II) model solutions was a peak at 2194 cm^{-1} which has been assigned to the CN stretch for a cyanate ligand complexed to a Cu(II) metal center, i.e. $[Cu(II)(NCO)_4]^{2-}$ complex ion.[31] For the Cu(I) model solutions, a peak was observed at 2220 cm^{-1} (see Table III and Figure S3). This demonstrates that the solution species observed in the SNIFTIRS spectra is indeed a Cu(I) cyanate species, i.e. $[Cu(NCO)_2]^-$.

XANES of Cu/NCO⁻ systems in DMSO (electrochemically generated and model solutions).—XANES was used to provide more information on the Cu/NCO^- electrochemical systems. It is known that XANES spectra of copper-based systems may vary dramatically with co-ordination geometry due to the different possible orbital configurations ($4s^2\ 3d^9$ / $4s^1\ 3d^{10}$) that can be manifest. These configurations allow various electronic transitions to occur, which are evident in the XANES spectra as peaks near the absorption edge. The +1 and +2 valence states of Cu can be distinguished by a shift in the absorption edge.[32] Cu(II), in particular, with its d^9 electronic configuration, is strongly susceptible to Jahn Taller distortion[32] which leads to alterations in the geometry of ligands around the metal center. In isocyanato-copper(II) complexes, coordination numbers can be 4,5, or 6 and the geometry can be pseudo-octahedral, coplanar, pseudotetrahedral, tetragonal pyramidal or trigonal bipyramidal depending on the ligands involved and the way the crystal structure is packed in the solid.[33]

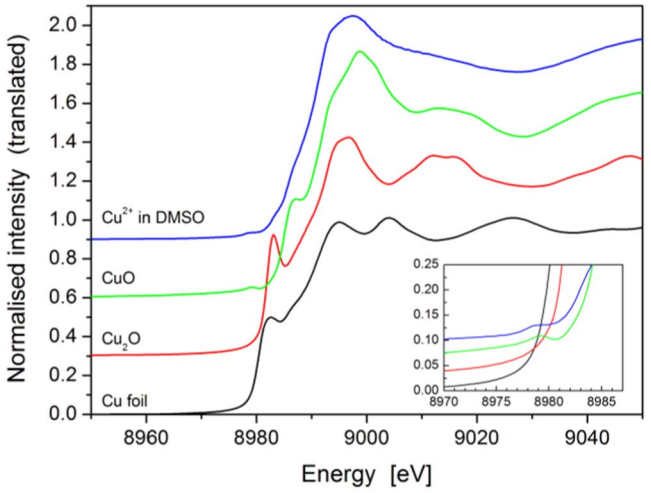

Figure 3. XANES spectra of Cu standards as labeled. The inset shows features in the pre-edge region. The spectra are normalized to a step height of 1 above the edge, and are subsequently offset for clarity.

Figure 3 shows the XANES spectra of the various standards measured, to which the sample spectra can be compared. Solid samples of Cu (foil), Cu_2O (powder) and CuO (powder) show characteristic features of these materials, namely for Cu_2O, a prominent peak at 8983 eV (the 1s-4p transition, indicative of Cu^+); and for CuO a small pre-edge peak at 8979 eV (the normally dipole-forbidden 1s-3d transition, indicative of Cu^{2+} with a break of inversion symmetry) and a peak at the leading edge that is less prominent than that of Cu_2O.

Cu^{2+} in DMSO was also measured as a standard in the form of a liquid N_2-frozen solution of partially oven dried $CuCl_2$ dissolved in DMSO. Its XANES spectrum was found to have a similar shape to XANES spectra run for other known octahedral Cu^{2+} species as reported by Huggins et al.[34] in that it exhibited a small pre-edge peak at 8979 eV, and had a single peak at the white line, in contrast to the two peaks observed in square planar and square pyramid complexes.[35]

Figure 4 shows XANES spectra of the model solutions and the electrochemically generated solution for the Cu/NCO^-/DMSO

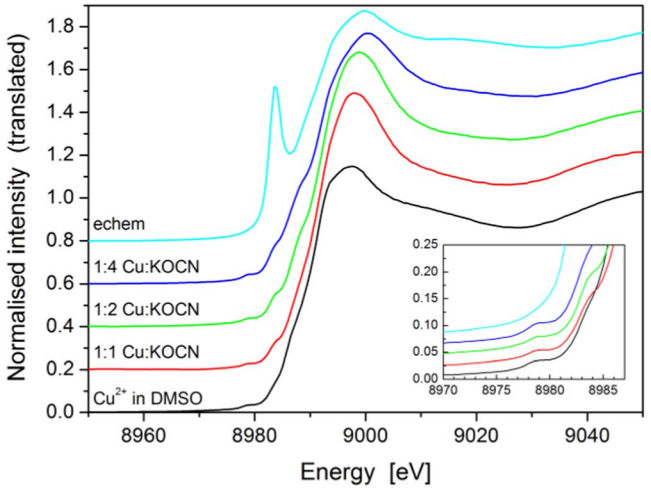

Figure 4. XANES scans of the model solutions prepared by adding Cu^{2+} and NCO^- in mole ratios of 1:1, 1:2 and 1:4, compared to a green-colored sample generated from the Cu/NCO^-/DMSO electrochemical system anodically polarized at +500 mV(AgCl/Ag) for 2 hours. The Cu^{2+} in DMSO standard is also shown for comparison. The inset shows the pre-edge region. The spectra are normalized to a step height of 1 above the edge, and are subsequently offset for clarity.

system. The shapes of the XANES spectra for the model solutions all closely resemble those for Cu^{2+} in an octahedral geometry[34–36] and were observed in the $CuCl_2$-in-DMSO standard. In addition, they show a very small pre-edge peak at 8979 eV, indicating the presence of Cu^{2+}.

In contrast, the electrochemically generated solution spectrum does not show a peak at 8979 eV, but instead has a very prominent feature at 8983.5 eV, which is in a similar position to the peak in the Cu_2O standard (8983.0 eV), and indicates the presence of Cu(I).[37] This peak, which corresponds to the 1s-4p transition, is more intense than in the Cu_2O standard and indicates Cu^+ is probably present in a 2-fold co-ordination environment.[37,38] This agrees with the IR and model solution data that the prominent Cu species present in solution is a Cu(I) cyanate complex.

As mentioned above, the XAS experiments focused on XANES data acquisition rather than full EXAFS due to the radiation sensitivity of the copper-containing solutions. Radiation hardness for the purpose of XANES was assessed by recording short (7 min) repeat spectra of the light green colored cell solution that was generated by polarizing the Cu electrode at +500 mV(AgCl/Ag) in 0.025 mol L^{-1} KOCN and 0.1 mol L^{-1} TBAP in DMSO for 1–2 hours. The results are summarized in Figure S4, showing signs of radiation damage after the first scan (intensity decrease of the peak at 8983.5 eV with the position remaining unchanged). Thus XANES spectra reported in this work are only the first scan of the series recorded for each sample.

Cu/NCS⁻ systems.— Figure 5 and Figure 6 show the CV, SNIFTIRS spectra, current/potential plots and IR intensity data pertaining to the Cu/NCS^- electrochemical systems in DMF and DMSO respectively.

CV investigations of the Cu/TBAP/NCS⁻/DMF and DMSO systems.— The CVs of the copper electrode in DMF and DMSO solvents containing 0.05 mol L^{-1} NCS^- and 0.1 mol L^{-1} TBAP are shown in Figure 5a and 6a. The CVs for this system were similar to the Cu/NCO^- electrochemical systems: largely featureless, but generally showing an increase in current as more anodic potentials were applied. In the anodic region of the CV, concurrent processes such as metal and solvent oxidation were jointly responsible for the increase in current in this region. In the Cu/DMF/NCS^- system (Figure 5a), the CV showed some hysteresis which indicated irreversibility of processes at the electrode.

IR spectra of Cu/TBAP/NCS⁻/DMF and DMSO.—Figure 5b and 6b show the series of SNIFTIRS spectra of the Cu/NCS^-/TBAP/DMF and DMSO systems acquired as a function of applied potential at the copper electrode surface. These were obtained after ratioing against a background spectrum recorded at −900 mV (AgCl/Ag). Figure 5c and 6c present the current/potential data plots showing the average current

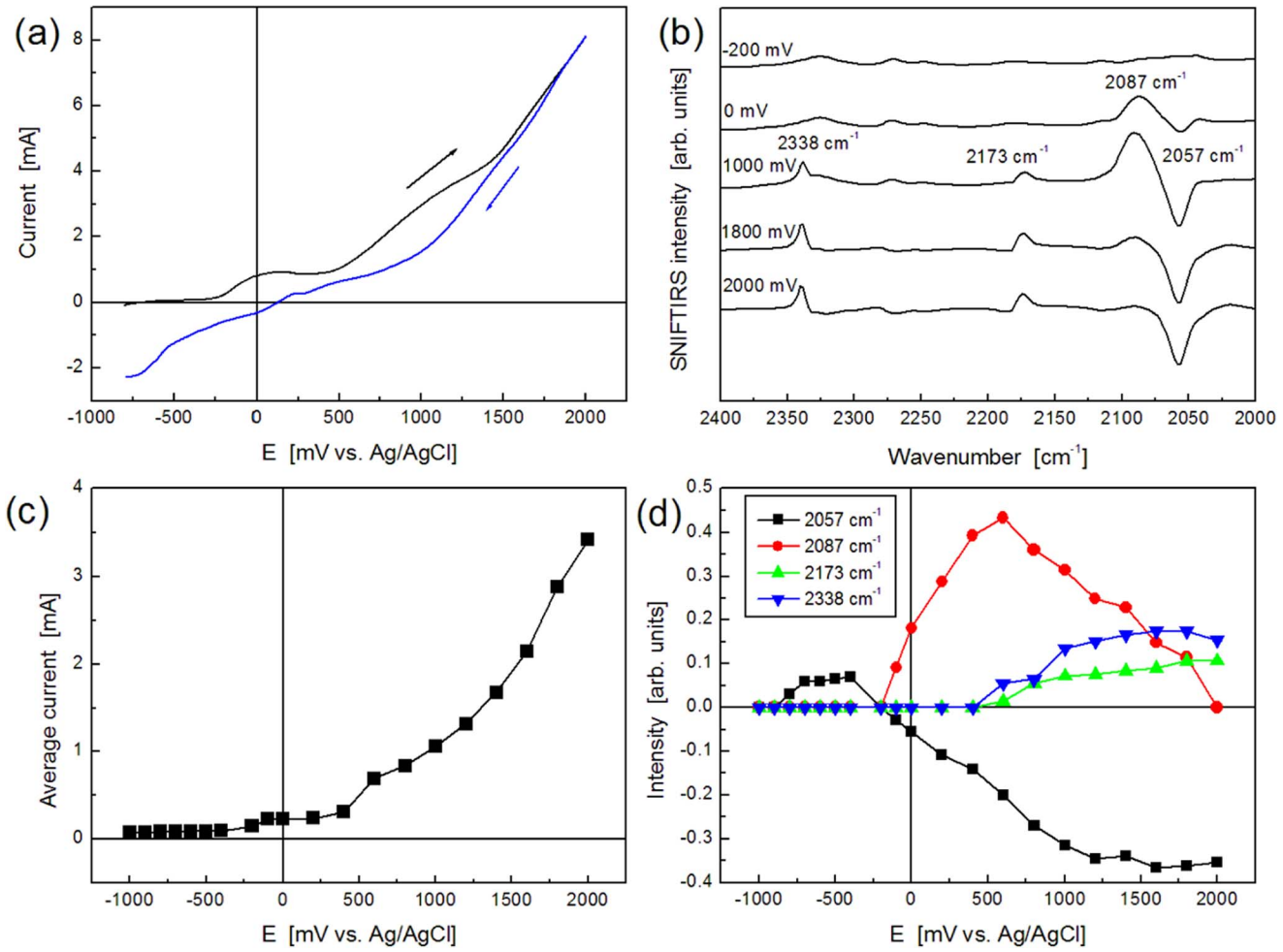

Figure 5. Combined electrochemical and SNIFTIRS-related data pertaining to the copper electrode system in DMF electrolyte containing 0.05 mol L^{-1} NaSCN and 0.1 mol L^{-1} TBAP: (a) CV (sweep rate = 20 mV/s, arrows show the path actually traced upon conducting the potential sweep), (b) SNIFTIRS spectra of the copper electrode as a function of applied potential, (c) Current/potential data acquired of the copper electrode during SNIFTIRS experiments (current was averaged at the beginning and end of the acquisition period for each applied potential), and (d) Intensity changes of SNIFTIRS peaks corresponding to the various molecular species generated in the thin layer from the copper electrode: free NCS^- (2057 cm^{-1}), Cu(I)/Cu(II)-NCS^- complex (2087 cm^{-1}), CuSCN solid film (2173 cm^{-1}), CO_2-DMF (2338 cm^{-1}).

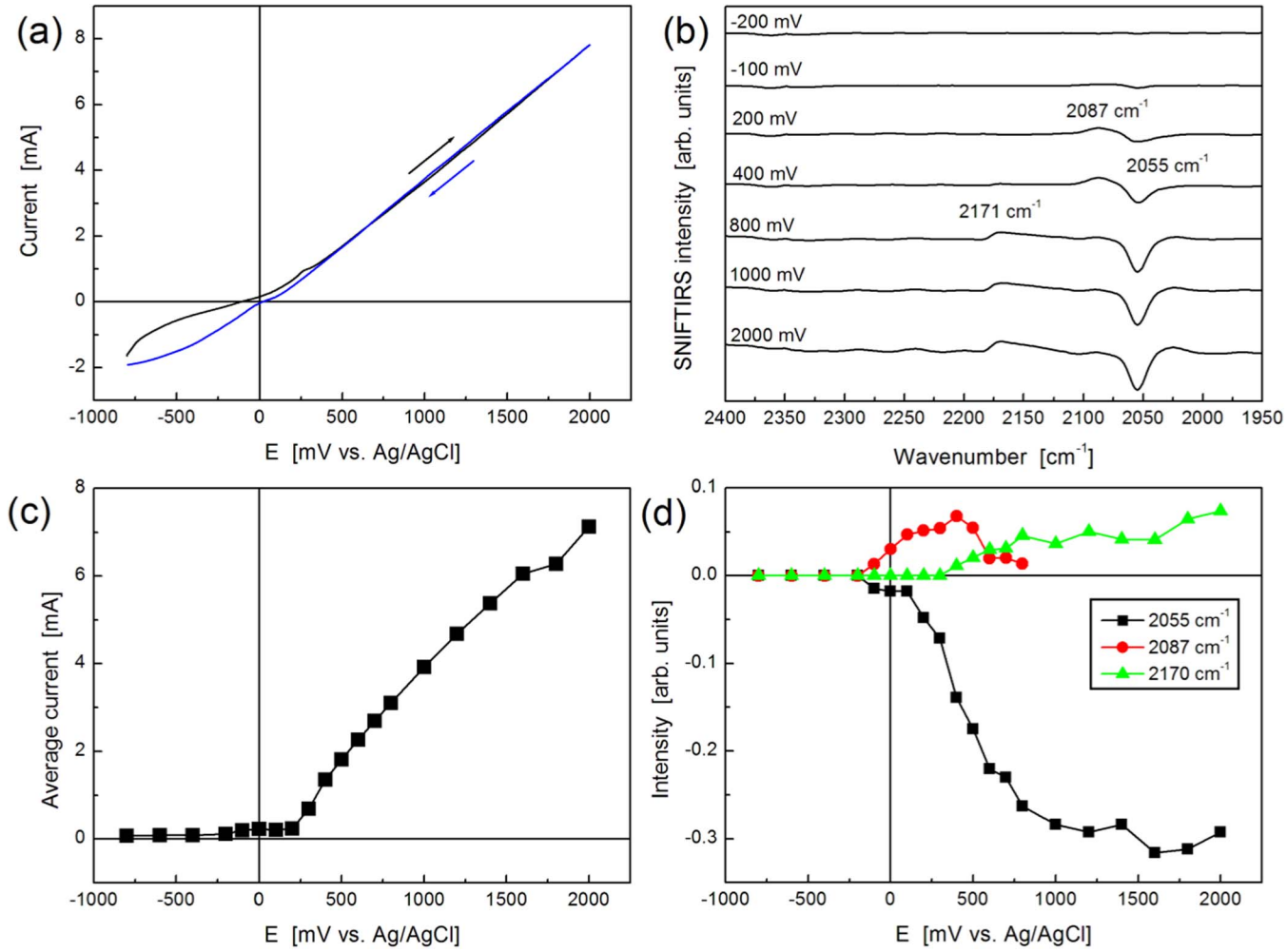

Figure 6. Combined electrochemical and SNIFTIRS-related data pertaining to the copper electrode system in DMSO electrolyte containing 0.05 mol L^{-1} NaSCN and 0.1 mol L^{-1} TBAP: (a) CV (sweep rate = 20 mV/s, arrows show the path actually traced upon conducting the potential sweep), (b) SNIFTIRS spectra of the copper electrode as a function of applied potential, (c) Current/potential data acquired of the copper electrode during SNIFTIRS experiments (current was averaged at the beginning and end of the acquisition period for each applied potential), and (d) Intensity changes of SNIFTIRS peaks corresponding to the various molecular species generated in the thin layer from the copper electrode: free NCS^- (2055 cm^{-1}), Cu(I)/Cu(II)-NCS^- complex (2087 cm^{-1}), CuSCN solid film (2170 cm^{-1}).

measured at each applied potential in the thin layer cell during the SNIFTIRS experiment. Figure 5d and 6d show the plots of the intensity changes of SNIFTIRS peaks observed in the Cu/TBAP/NCS^-/DMF and DMSO systems as a function of applied potential. Table I gives the frequencies of the IR peaks observed for both Cu/NCS^- systems studied.

In general, peaks of interest in the SNIFTIRS spectra of the Cu/NCS^- systems appeared at relatively less cathodic applied potentials than in the Cu/NCO^- SNIFTIRS spectra. Four features of interest appear in the SNIFTIRS spectra for the Cu/NCS^- electrochemical systems (Figure 5b, 6b): at 2055–2057, 2087, 2171–2173 and 2338 cm^{-1}. The spectrum acquired at −200 mV(AgCl/Ag) shows only solvent related peaks due to DMF. At applied potentials between −100 mV and 0 mV(AgCl/Ag), a negative-going peak at 2055–2057 cm^{-1} and a broad positive-going peak at 2087 cm^{-1} are observed. The negative peak at 2055–2057 cm^{-1} is due to free thiocyanate ion, as identified in earlier in situ IR spectroscopy work involving the Ni/NCS^-/DMSO or DMF systems.[13] The peak at 2087 cm^{-1} has been observed in earlier non-electrochemical studies by other workers and has been subject to various interpretations.[10,39,40] Forster and Goodgame reported IR data (run as nujol mulls) of a $(C_2H_5)_4N[Cu(NCS)_4]$ salt which showed a strong ν(CN) stretching frequency at 2074 cm^{-1}. The solid was described as being either green or purple depending on the counter cation used to precipitate the solid[39] but dissolved in nitromethane or acetone to produce characteristic blood red solutions, for which no IR data were reported. In the present study, a red solution *was* observed to develop over time in the thin layer cell during the in situ IR experiment. Given literature reports, the characteristic red coloration must indicate the presence of a complex of Cu^{2+} and NCS^- ion., The exact identity of the copper/thiocyanate species detected in the present study, has been discussed by various authors and attributed to differing species. Rannou et al.[40] who studied the dissolution of "CuSCN" solutions in various polar aprotic solvents (including DMSO) reported a peak at 2089 cm^{-1} for saturated ($\sim 10^{-2}$ mol L^{-1}) solutions of CuSCN in DMSO which they assigned to a copper-isothiocyanate ion-pair "Cu^+NCS^-" because it was thought that the Cu^+ ion would be poorly solvated by oxygen donors provided by these solvents. However, work performed in the present study involving model solutions (Cu/NCS-/DMF or DMSO model solutions section) disputes that earlier judgment by Rannou et al. Model solutions prepared from mixing cupric chloride and NCS^- in DMSO or DMF in a 1:1 to 1:8 mole ratio for Cu^{2+}:DMSO (and 1:1 to 1:4 for Cu^{2+}:DMF) produced red to intense red solutions, and the transmission IR spectra featured a peak over the 2084–2093 cm^{-1} range, which includes the 2089 cm^{-1} value reported by Rannou et al.[40] These peaks were very broad, suggesting that there may be a mixture of copper-thiocyanate complex

ions present with Cu being in different oxidation states but having similar ν(CN) stretching frequencies. Indeed, later work reported by Bowmaker et al.[10] supports this suggestion. In that study, complexes of $[AsPh_4]M(SCN)_2$ and $N(PPh_3)_2[M(SCN)_2]$ (M=Cu(I) or Au(I)) were prepared and characterized by IR spectroscopy as nujol mulls and when dissolved in tributylphosphate solvent. In the nujol mull (solid state) spectra, two strong peaks were observed at 2105–2109 and 2084 cm^{-1} due to ν(CN) stretching; however, in tributyl phosphate solutions, only one peak was observed, centered at 2085 cm^{-1}, which is similar in position to the peak observed in the present study, at 2087 cm^{-1} (see Figure 5b and 6b). Bowmaker et al. attributed this peak to the discrete complex ion species $[Cu(SCN)_2]^-$. We believe this Cu(I) thiocyanate complex ion species contributes to the SNIFTIRS peak observed at this frequency in both Cu/NCS^- electrochemical systems studied. However, the red color observed in the cell solution after the in situ IR experiment cannot be attributed to a Cu(I) thiocyanate complex, as these are known to be colorless (see Cu/NCS-/DMF or DMSO model solutions section). Instead the red color must be due to the presence of additional Cu(II) thiocyanate complexes which would have formed in the electrochemical cell at more anodic potentials.[41]

Another weak, broad peak, centered at ca. 2173 cm^{-1} (in systems with DMF) and 2170 cm^{-1} (in systems with DMSO) respectively, is observed in Figure 5b and 6b. This peak at 2170–2173 cm^{-1}, believed to be due to the same species in both systems, has been attributed to a solid film deposited on the Cu electrode. Spectral evidence that the peak was due to a solid species was demonstrated by acquiring IR transmission spectra of the red-colored cell solution extracted from the thin layer cell after conducting the SNIFTIRS experiment. These spectra featured a peak at 2087 cm^{-1} and no peak at 2170–2173 cm^{-1}, which proved that the former peak is due to solution species (i.e. a mix of Cu(I) and Cu(II) complex ions with thiocyanate), while the latter peak must be due to a solid film which would have deposited on the electrode surface.

The nature of this solid electrodeposited film giving the SNIFTIRS peak at 2170–2173 cm^{-1} in the Cu/NCS^- electrochemical systems is uncertain but is likely a solid "CuSCN" species. This assignment is supported by work reported by Kilmartin et al.[8] who studied the formation mechanism of electrochemically deposited copper thiocyanate films on a copper anode, in which he assigned a Raman peak observed at 2175 cm^{-1} to an underlying CuSCN barrier film.

Other workers reporting spectroscopic data for CuSCN[10,40,42] have also reported peaks at 2173 cm^{-1}. These studies have suggested what the nature of the solid CuSCN film on the Cu electrode in the present study could be. Clark et al.[42] reported the IR spectrum of solid CuSCN to have a strong ν(CN) stretching peak at 2165 cm^{-1} which was assigned to S-bonded CuSCN. However, he also attributed a weak shoulder at 2173 cm^{-1} in the same spectrum to a bridge-bound Cu(I) species with thiocyanate. Kabesova et al.[43] discussed the effect of bridged thiocyanates on copper/thiocyanate compounds in IR spectra. They report that the infrared spectrum of "CuNCS" features a peak at 2173 cm^{-1} due to ν(CN) stretching, and that the mode of bridging present in this compound occurs involves Cu-N and Cu-S bonds. Hence it is possible that the solid film on the electrode in the present study could contain some bridged structures.

The only other species to be detected in SNIFTIRS spectra of the Cu/NCS^- electrochemical systems (and only in DMF-based electrolytes, Figure 5b) was a peak at 2338 cm^{-1}, which can be attributed to dissolved CO_2 species in the DMF electrolyte. This species may arise from oxidation of either the pseudohalide ion or the DMF solvent. Its appearance solely in the DMF-based electrolyte (Figure 5b) mirrored the trend observed in the Cu/NCO^- system (IR spectra of Cu/TBAP/NCO-/DMF and DMSO section) where CO_2 formation in the DMSO-based electrolyte was also not observed.

Cell current data (from current/potential plots) and the trending of intensities of detected electrogenerated species with respect to the cell current for SNIFTIRS-detected species in the thin layer as a function of applied potential in the Cu/NCS^-/DMF or DMSO electrochemical systems studied show consistent behavior (see Figure 5c, 5d, 6c and 6d). The intensity of the peak at 2055–2057 cm^{-1} (attributed to the free NCS^- ion in the solvent) is negative for all applied potentials at the electrode studied apart from SNIFTIRS spectra recorded at −800 to −100 mV(AgCl/Ag) in the Cu/DMF/NCS^- electrochemical systems. In both DMF and DMSO-based systems, the intensity of the peak due to free NCS^- ion becomes increasingly negative in the applied anodic potential region, where there is an obviously stronger demand (as can be deduced from the current/potential data in Figure 5c and 6c) for free thiocyanate ion to form soluble Cu(I)/Cu(II) complexes, solid deposited films and electrogenerated CO_2. This is supported by the fact that there is an increase in the intensity of peaks due to the soluble Cu(I) and Cu(II) thiocyanate complex ion species (broad peak at 2087 cm^{-1} in both systems), with increases beginning between −400 and −200 mV(AgCl/Ag), and reaching a maximum at +400-600 mV(AgCl/Ag) in the anodic applied potential region, before dropping off. The decrease in intensity of the 2087 cm^{-1} peak is accompanied by an increase in intensity of peaks at 2170–2173 cm^{-1} and 2338 cm^{-1}, which are due to solid CuSCN film deposits and solvent-dissolved CO_2 respectively. This shows that film deposition is occurring as a result of limited solubility in the thin layer cell of the copper/thiocyanate complex ions formed in the solvents used (DMSO and DMF). At the highest potentials applied in the SNIFTIRS experiment, the intensities due to the deposited CuSCN film and electrogenerated CO_2 level off and increase only gradually as increasingly anodic potentials are applied.

Cu/NCS^-/DMF or DMSO model solutions.—As for the Cu/NCO^- electrochemical studies, the identity of solution species detected in the in situ IR experiments involving NCS^- was proven by preparing model solutions in DMSO by mixing cupric chloride or cuprous iodide salts with sodium thiocyanate. Figure 7 summarize IR transmission spectra of these model solutions while Table II and Table III summarize the IR assignments deduced from Figure 7.

It is necessary to elucidate and prove the identity of the Cu-based complex ion that gives rise to the 2087 cm^{-1} peak observed in SNIFTIRS spectra of the Cu/NCS^- electrochemical systems in DMF and DMSO. When solutions of $CuCl_2$ and NCS^- in DMF or DMSO are mixed together, they form a characteristic blood red solution, which is the typical color of Cu(II)-thiocyanate complex ion species is reasonable.[44] Two peaks detected from IR transmission spectra of these model solutions were observed at ∼2055 and ∼2090 cm^{-1} (Figure 7). The peak observed at 2055–2056 cm^{-1}, which increases in intensity with increasing mole ratio, is due to the free NCS^- ion. The peak at ∼2090 cm^{-1} is due to the Cu^{n+}-thiocyanate complex ion species in solution. Although this appears to prove the identity of the peak observed in the SNIFTIRS spectra, it is important to note that the model solution IR spectra reveal some fortuitous complexity which actually aid in confirming the assignment of the SNIFTIRS-detected peak at 2087 cm^{-1} in the Cu/NCS^- electrochemical systems to a Cu(I) *and* Cu(II) thiocyanate-complex ion species.

In Figure 7, it is seen that as the mole ratio ($CuCl_2$:NaSCN) was increased from 1:1 to 1:4, the peak maximum of the ν(CN) stretch attributed to the Cu^{n+}-thiocyanate complex ion species decreased from 2093 to 2091 cm^{-1} in DMSO and from 2090 to 2084 cm^{-1} in DMF. The shift is caused by redox chemistry[44] occurring in the model solution which produces a Cu(I) thiocyanate species from reduction of the Cu(II) ion by NCS^- ion. The redox process is encouraged by addition of more NCS^- ion relative to the $CuCl_2$ salt. Figure 7 shows that the ν(CN) stretching frequency shifts *toward* values observed in CuI/NaSCN mixtures where Cu(I) thiocyanate complexes should form directly. The redox process does not occur when Cu(I) salts are mixed with NCS^-. Furthermore, CuI/pseudohalide salt model solution mixtures are green to colorless, not red, which confirms that Cu(II) is absent as expected. In the $CuCl_2$/NaSCN model solution mixtures, in contrast, a mixture of the two oxidation states of Cu exists, with the color of the solution dominated by that due to the Cu(II) thiocyanate complex ions. The broad shape of the peaks provides further evidence to support the hypothesis that there is a mixture of the Cu(I) and Cu(II) thiocyanate complexes in the $CuCl_2$/NaSCN model solutions. A comparison of $CuCl_2$/NaSCN and CuI/NaSCN model solution IR

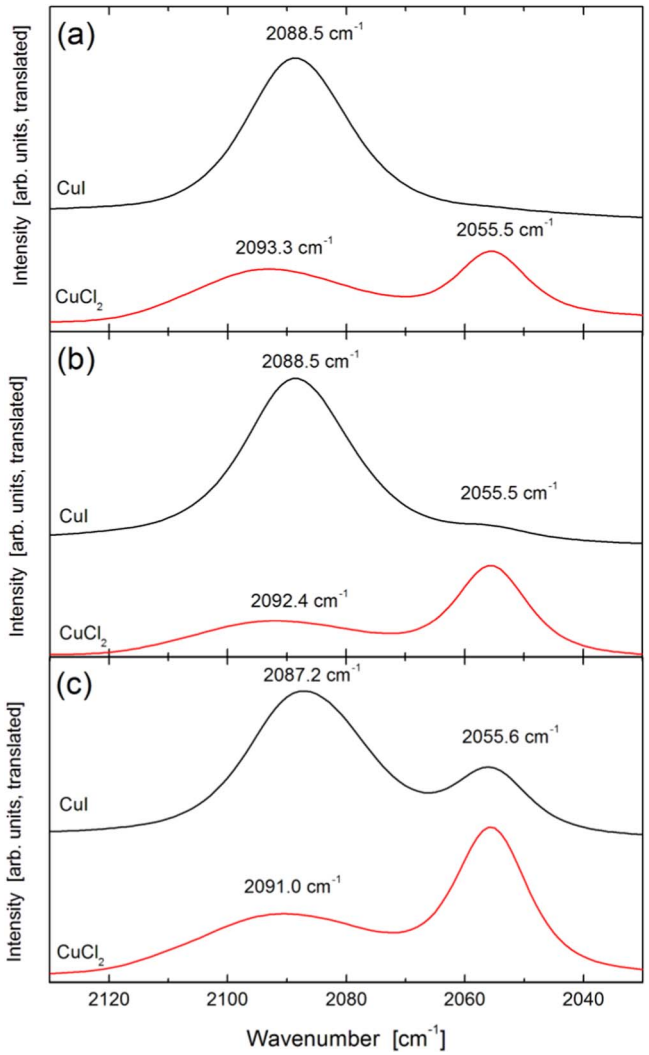

Figure 7. Transmission IR spectra of Cu(I) and Cu(II) pseudohalide complexes in the model solutions prepared with CuI and $CuCl_2$ salts at different mole ratios of Cu salt:pseudohalide salt in NaSCN salt/ DMSO model solution, where [CuI] or [$CuCl_2$] = 0.025 mol L^{-1} in each solution. (a) 1:1 CuI: NCS^- and 1:1 $CuCl_2$: NCS^- mole ratio solutions, (b) 1:2 CuI: NCS^- and 1:2 $CuCl_2$: NCS^- mole ratio solutions, (c) 1:4 CuI: NCS^- and 1:4 $CuCl_2$: NCS^- mole ratio solutions.

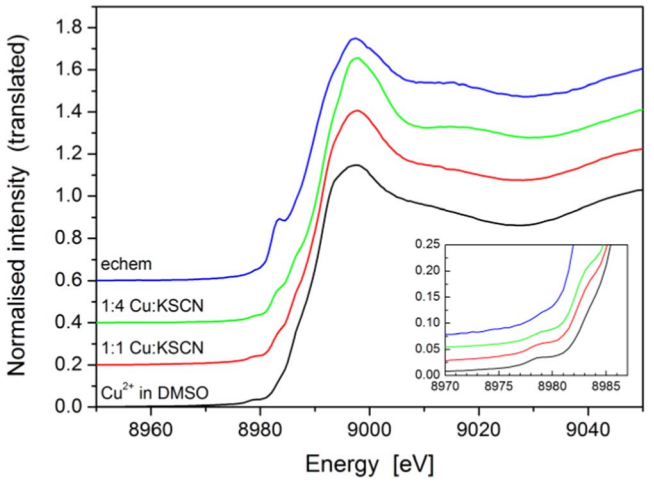

Figure 8. XANES scans of the model solutions prepared by adding Cu^{2+} and NCS^- in mole ratios of 1:1 and 1:4, and of the solution generated from the Cu/NCS^-/DMSO electrochemical cell system (produced by polarizing the electrode at 200 mV for 2–3 hours). The Cu^{2+} in DMSO standard is also shown for comparison. The inset shows the pre-edge region. The spectra are normalized to a step height of 1 above the edge, and are subsequently offset for clarity.

spectra at the different mole ratios is shown in Figure 7. It is clear that the ν(CN) stretch peak of the Cu(I) species near 2090 cm^{-1} was narrower than that for the Cu(II) salt/pseudohalide solutions, hence this constitutes further evidence that only one oxidation state of Cu must exist in the Cu(I) model solutions.

The fortuitous redox chemistry observed in the model solutions hence serves to illustrate the situation that occurs in the cell solution during electrical polarization of Cu electrodes in the NCS^-containing electrolytes in the SNIFTIRS experiment, i.e. *two* oxidation states of copper exist in it. This is indicated by 1) the red color that develops in the cell solution during the SNIFTIRS experiment, which must represent a Cu(II) thiocyanate species; and 2) the single, broad peak at 2087 cm^{-1} (see Figure 5b and 6b). Although a peak at this wavenumber value had previously been attributed to a Cu(I)-thiocyanate species[10] it is more likely, by reason of its innate broadness, to be due to overlapping contributions from Cu/thiocyanate complex ions existing in *two* oxidation states (i.e. Cu(I) and Cu(II)), which have ν(CN) stretching frequencies of only slightly different values.

XANES of Cu/NCS^- systems in DMSO (electrochemically generated and model solutions).—XANES spectra of the Cu/NCS^-/DMSO system as shown in Figure 8 for the model and electrochemical solutions provided supporting evidence to conclusions discussed above. The model solution Cu/NCS^-/DMSO XANES system spectra showed a small peak at 8979 eV, a small shoulder on the edge, and a single white line. These were all indicative of Cu^{2+} in an octahedral geometry in the samples.

A shoulder observed at 8982 eV (see Figure 8), however, illustrates that there is also some Cu(I) present in the model solutions. The electrochemically generated solution "echem" exhibited a small peak at 8979 eV and a peak on the edge at 8983 eV, while the white line and subsequent features mirrored those of the model solutions, indicating a mixture of Cu(I) and Cu(II), with a higher Cu(I) content than the model solutions. This hence corroborates the earlier discussed IR evidence from studies performed on the Cu(II) salt/pseudohalide salt mixtures discussed above. It also agrees with the observed red color that develops in the cell solution during the in situ IR experiment. Hence, XANES and IR studies of the electrochemical systems and the model solutions confirm that a mixture of Cu(I) and Cu(II) pseudohalide complex ions are generated in the electrochemical cell.

Cu/$NCSe^-$ systems.— Figure 9 and 10 show the CV, SNIFTIRS spectra, current/potential plots and IR intensity data pertaining to the Cu/$NCSe^-$ electrochemical systems in DMF and DMSO respectively.

CV investigations of the Cu/TBAP/$NCSe^-$/DMF and DMSO systems.—The CVs of the copper electrodes in DMF and DMSO containing 0.05 mol L^{-1} KSeCN and 0.1 mol L^{-1} TBAP are shown in Figure 9a and 10a. As observed for the other electrochemical systems, the CVs for these systems are also featureless, showing a monotonic increase in current as the applied voltage was adjusted from cathodic to anodic potentials. However, in contrast to the other systems, the CV for the Cu/$NCSe^-$ systems has significant hysteresis, which indicates irreversibility in both systems. This is possibly caused by loss of solid from or modification of the electrode by deposition of a film on the surface. The solid could be $K(SeCN)_{3(s)}$, as discussed later.

IR spectra of Cu/TBAP/$NCSe^-$/DMF and DMSO.—Figure 9b and 10b show the SNIFTIRS series acquired as a function of applied potential at the copper electrode surface for the Cu/$NCSe^-$/DMF and DMSO systems. Figure 9c and 10c illustrate the average current in the thin layer cell during the SNIFTIRS experiment in DMF and DMSO at each applied potential. Figure 9d and 10d are plots of the intensity changes of peaks observed in the Cu/TBAP/$NCSe^-$/DMF and DMSO

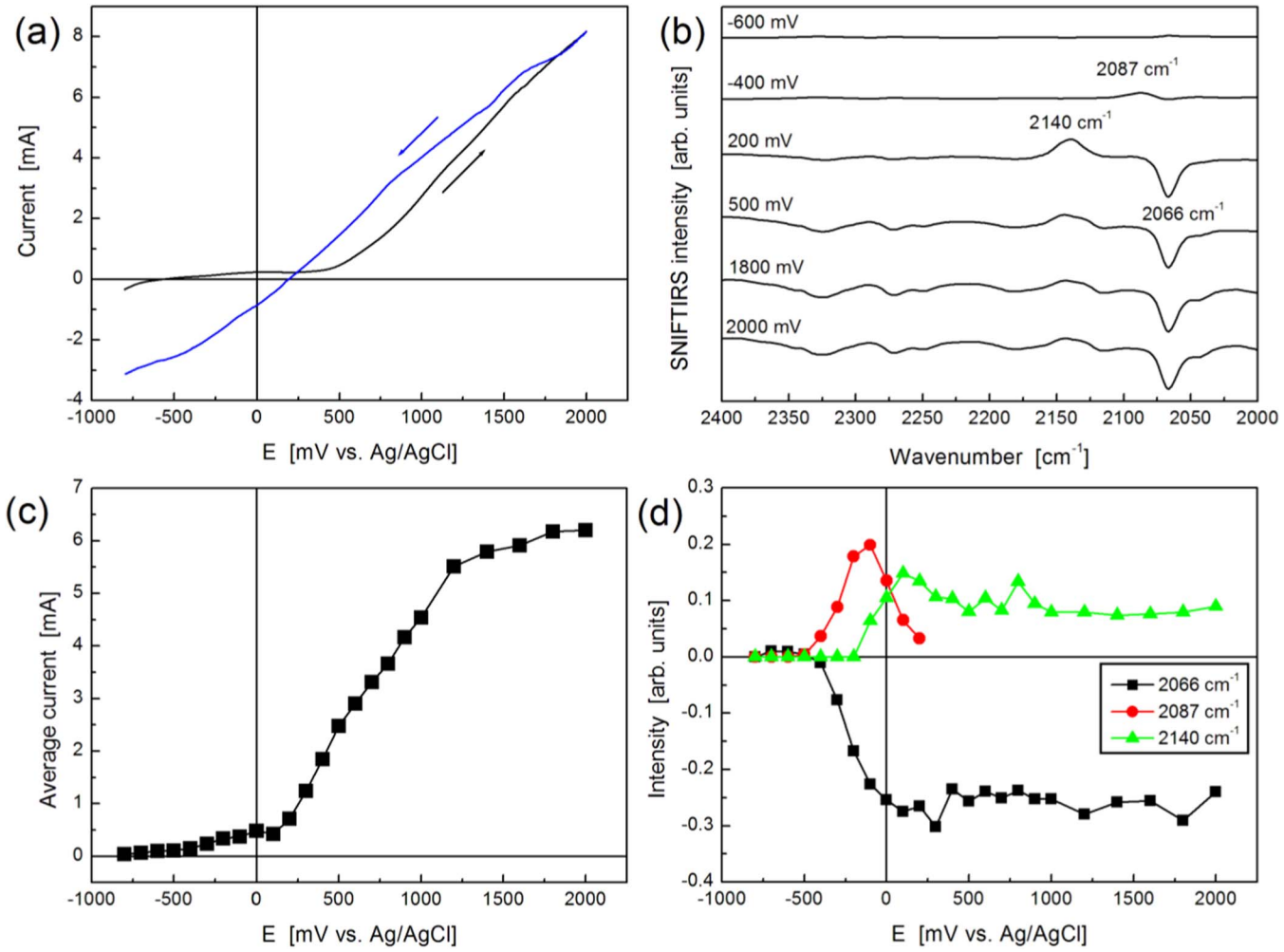

Figure 9. Combined electrochemical and SNIFTIRS-related data pertaining to the copper electrode system in DMF electrolyte containing 0.05 mol L^{-1} KSeCN and 0.1 mol L^{-1} TBAP (a) CV (sweep rate = 20 mV/s, arrows show the path actually traced upon conducting the potential sweep), (b) SNIFTIRS spectra of the copper electrode as a function of applied potential, (c) Current/potential data acquired of the copper electrode during SNIFTIRS experiments (current was averaged at the beginning and end of the acquisition period for each applied potential), and (d) Intensity changes of SNIFTIRS peaks corresponding to the various molecular species generated in the thin layer from the copper electrode: free $NCSe^-$ (2066 cm^{-1}), Cu(I)/Cu(II)-NCSe- complex (2087 cm^{-1}), $K(SeCN)_3$ (2140 cm^{-1}).

systems respectively as a function of applied potential. A summary of the SNIFTIRS data is given in Table I.

Three features were observed in the SNIFTIRS spectra of the $Cu/NCSe^-$ systems at 2065–2066, 2087–2089, and 2138–2140 cm^{-1}. The broad positive-going peak at 2087–2089 cm^{-1} and the negative-going peak at 2065–2066 cm^{-1} occur at applied potentials between −400 mV and + 500 mV (AgCl/Ag) in Figure 9b and 10b. This pattern of peaks is analogous to that observed in the Cu/NCS^-/DMF and Cu/NCS^-/DMSO systems, and can be interpreted similarly: the negative-going peak at 2065–2066 cm^{-1} is due to free selenocyanate ion and the broad positive-going peak at 2087–2089 cm^{-1} is likely a mixture of Cu(I) and Cu(II) selenocyanate complex ions, assuming a similar chemistry to the Cu/NCS^- systems. Since data on Cu-selenocyanate complex ion systems are lacking in the literature, it was difficult to confirm the assignment of the 2087–2089 cm^{-1} peak observed in Figure 9b and 10b to a Cu^{n+}- selenocyanate complex ion species. The most useful study which lends support to the assignment of the 2087–2089 cm^{-1} peak to Cu^{n+}-selenocyanate complex ion species is a comprehensive review by Bailey et al.[45] which states that the ν(CN) stretching frequency of "$CuL_2(SeCN)_2$" (L = N,N,diethyl 1,2-diaminoethane) in a nujol mull is 2072 cm^{-1}. This is regarded by the authors as the typical IR stretching frequency for "apparently N-bonded" Cu-NCSe complexes, while Se-bonded (Cu-SeCN) analogues give higher ν(CN) stretching frequencies. Hence in Figure 9b and 10b, the assignment of the observed 2087–2089 cm^{-1} band to Cu^{n+}- selenocyanate complex ion species is reasonable. According to Norbury,[46] Cu can bond via the N or the Se atom in the $SeCN^-$ ligand. It is also stated by Norbury that complexes of $Cu(en)_2(SeCN)_2$ are probably isostructural with the equivalent NCS^- based complexes.

The color of the SNIFTIRS cell solutions (after or during electrical polarization of the Cu electrode in KSeCN/DMSO or KSeCN/DMF electrolytes) could not be used (as it could with the Cu/thiocyanate ion electrochemical systems) to visually characterize whether or not Cu(I) or Cu(II) existed in solution. In general, both DMF and DMSO cell solutions in the Cu electrode systems after extensive anodic polarization ended up being gold-yellow in color. Such colors were also obtained in model solution preparations where $CuCl_2$ and CuI salts were mixed with the pseudohalide salts in various copper salt: pseudohalide salt mole ratios (see Table II). Other evidence was sought to identify the oxidation states of Cu present in the solutions.

In addition to the peak at 2087–2089 cm^{-1}, another peak that appears in the SNIFTIRS spectra (see Figure 9b and 10b) is a weak, broad feature at 2138–2140 cm^{-1}. This feature is observed at applied potentials of +200 (±100) mV upwards for Cu electrodes in DMF solutions, and from +600 mV (±100) mV upwards for Cu electrodes in DMSO solutions. IR transmission spectra of the cell

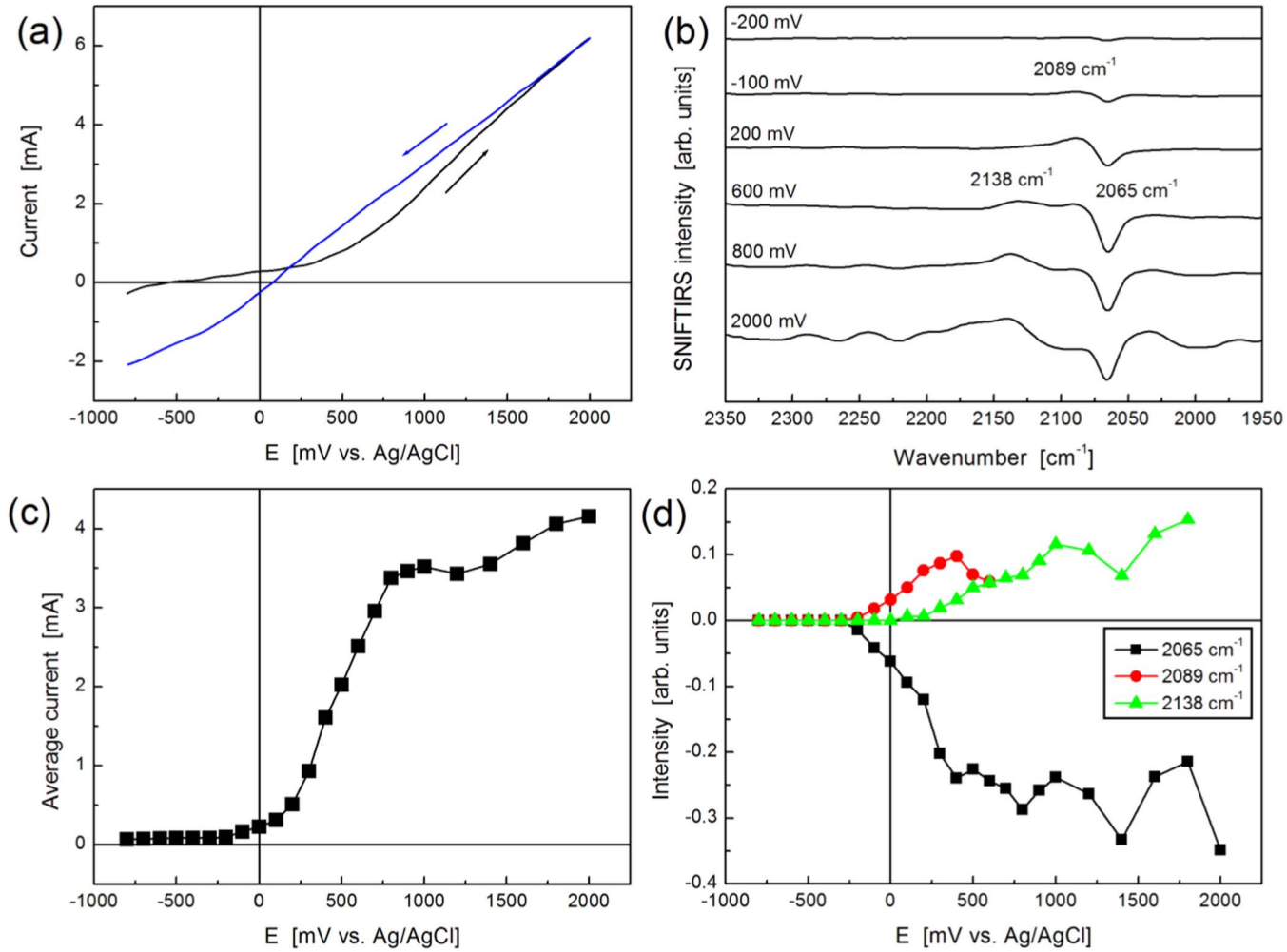

Figure 10. Combined electrochemical and SNIFTIRS-related data pertaining to the copper electrode system in DMSO electrolyte containing 0.05 mol L^{-1} KSeCN and 0.1 mol L^{-1} TBAP (a) CV (sweep rate = 20 mV/s, arrows show the path actually traced upon conducting the potential sweep), (b) SNIFTIRS spectra of the copper electrode as a function of applied potential, (c) Current/potential data acquired of the copper electrode during SNIFTIRS experiments (current was averaged at the beginning and end of the acquisition period for each applied potential), and (d) Intensity changes of SNIFTIRS peaks corresponding to the various molecular species generated in the thin layer from the copper electrode: free $NCSe^-$ (2065 cm^{-1}), Cu(I)/Cu(II)-$NCSe^-$ complex (2089 cm^{-1}), $K(SeCN)_3$ (2138 cm^{-1}).

solutions obtained after performing SNIFTIRS experiments on the Cu/KSeCN system in DMSO only show peaks at 2088 cm^{-1} and 2065 cm^{-1}, which are known and assigned solution species. The peak at 2138–2140 cm^{-1} is not observed under these conditions, thus proving it must be a solid phase species existing as a film deposited on the Cu electrode. Although this was initially thought to be due to a solid film of CuSeCN, spectroscopic data from the literature prove otherwise. Kilmartin et al.[11] attributed a weak band (detected by Raman spectroscopy) at 2164 cm^{-1} to a copper selenocyanate passive film that had formed on a copper anode. Assuming a low point group symmetry of CuSeCN, the detected 2164 cm^{-1} peak (in Kilmartin's work) would be expected to be observed at the same position in IR spectroscopy. This is reasonably distant in value from the observed peak of 2138–2140 cm^{-1} in the present IR spectroelectrochemical study. Manceau et al.[47] reported data relating to ν(CN) stretching frequencies of various thiocyanate and selenocyanate compounds. The ν(CN) stretching frequencies of α-CuSCN, β-CuSCN, α-CuSeCN, and β-CuSeCN are reported at 2157, 2173, 2157 and 2174 cm^{-1} respectively, which are all very similar to Kilmartin et al.'s observed peak.[11] Manceau et al.[47] stated that these IR frequencies were more typical of Cu-Se bonded compounds. Hence the 2138–2140 cm^{-1} peak is unlikely to be due to a Cu-$SeCN^-$-containing solid compound, hence other candidate species must be considered. It is known that selenocyanogen ($Se_2(CN)_2$) can be isolated as a yellow solid from dichloromethane where it is formed by reaction of silver selenocyanate with iodine. Aynsley et al.[48] reported that the yellow chloroform (or benzene) solutions of selenocyanogen exhibit ν(CN) stretching frequencies of 2152 cm^{-1}, while Cataldo,[49] who reported the first IR spectrum of *solid* selenocyanogen (as a KBr disk), stated that a very intense ν(CN) stretching frequency can be observed in the FTIR spectra at 2143 cm^{-1}. Burchell et al.[50] studied the series of molecules $Se_x(CN)_2$ (x = 1–3) and reported spectroscopic and structural data. The observed ν(CN) stretching frequencies for both $Se_2(CN)_2$ and $Se(SeCN)_2$ were reported as being at 2144 cm^{-1}. We therefore speculate from this previous literature evidence that the peak could be due to an $(NCSe)_3^-$ species, because this species is thermodynamically favored when in equilibrium with its progenitor species $(SeCN)_2$ and $NCSe^-$, according to Solangi et al.[51] In the presence of K^+ ion (from the use of KSeCN), the $(SeCN)_3^-$ ion may precipitate and become "trapped" in this form as a $K(SeCN)_3$ film on the electrode. This compound is known from earlier studies[9] involving the oxidation of selenocyanate on platinum electrodes in aqueous electrolytes containing 0.5 mol L^{-1} KSeCN and 0.1 mol L^{-1} NH_4O_2CMe at pH 7 and was attributed to an intense band at 2143 cm^{-1} that was observed when applied potentials >0.8 V (NHE) were used. We therefore propose that the peak at 2138–2140 cm^{-1} is due to a film of $K(SeCN)_3$ on the Cu electrode.

In contrast to the Cu/NCO^- and Cu/NCS^- systems, no peak at 2338 cm^{-1} was observed in any of the SNIFTIRS spectra of the Cu/$NCSe^-$ electrochemical systems in either DMF and DMSO. Its absence may be due to the copper electrode surface becoming poisoned or blocked during the polarization at anodic potentials by a layer of solid $K(SeCN)_3$ which may inhibit electrochemical surface reactions. Selenocyanate compounds or derivatives are known to decompose to elemental Se[9,11] which may inhibit surface reactions. At the conclusion of any SNIFTIRS experiments involving Cu electrodes in $NCSe^-$, the surface of the Cu electrode was noted to be black in color, comprising physical proof that a film had deposited during the experiment.

The cell current/potential plots and intensity-potential plots for the Cu/$NCSe^-$/DMF and DMSO electrochemical systems studied by in situ IR are shown in Figure 9c, 10c, 9d and 10d respectively. Very similar intensity trends in species were observed for the Cu/DMSO/$NCSe^-$ electrochemical system (Fig. 10d) when compared to that of Cu/DMSO/NCS^- (Figure 6d). However, the Cu/DMF/$NCSe^-$ electrochemical system (Figure 9d) showed more activity in the −500 mV to 0 mV(AgCl/Ag) region relative to its Cu/DMF/NCS^- counterpart (Figure 5d). The intensity of the Cu-selenocyanate complex ion species (observed at 2087–2089 cm^{-1}) increased to a maximum value at −100 mV and +400 mV(AgCl/Ag) in the DMF and DMSO systems respectively. The intensity of the 2138–2140 cm^{-1} peak, attributed to the deposited $K(SeCN)_3$ on the electrode, was noted to increase as the intensity of the 2087–2089 cm^{-1} peak began to drop, and plateaued at more anodic applied potentials. Also in common with all the Cu/NCO^- and Cu/NCS^- electrochemical systems investigated by SNIFTIRS in DMF and DMSO, the intensity of the peak at 2065–2066 cm^{-1} (due to free selenocyanate ion) decreased sharply to increasingly negative intensities. This corresponded to the consumption of selenocyanate ion in the thin layer cell while the Cu electrode was being polarized, with sharper drops being observed at earlier applied potentials in the more electrochemically active Cu/DMF/$NCSe^-$ system (see Figure 9d). At mid to high anodic applied potentials, fluctuations in intensities of the peak due to free selenocyanate ion were observed. This suggested the occurrence of "thin layer turbulence", which is interpreted as being caused by gas production during the experiment. In the case of the Cu/$NCSe^-$/DMF or DMSO systems it was not obvious what gas was causing this problem as CO_2 was not observed in the in situ IR spectra at any applied potential.

Cu/$NCSe^-$/DMF or DMSO model solutions.—Model solutions were prepared to specifically prove the identity of the peak at 2087–2089 cm^{-1}, attributed in the discussion above to a Cu^{n+}-selenocyanate complex ion species. As shown in Table II, mixing DMF and DMSO solutions of Cu^{2+} and $NCSe^-$ in different Cu^{2+}:$NCSe^-$ mole ratios produced gold yellow colored solutions. Increasing the Cu^{2+}:$NCSe^-$ mole ratio from 1:1 to 1:8 resulted in an increase of the intensity of the color to an orange brown color (c.f. the Cu^{2+}/$NCSe^-$ model solution series discussed earlier). This color was similar to (although it was more intense than) the cell solution color observed in the Cu/$NCSe^-$ electrochemical systems during the SNIFTIRS experiments. The transmission IR spectra of the DMF model solutions containing Cu^{2+} and $NCSe^-$ featured a peak at 2065–2066 cm^{-1} and a peak at 2084–2090 cm^{-1} (for which the position decreased in wavenumber value as the Cu^{2+}:$NCSe^-$ mole ratio was increased from 1:1 to 1:4). The peak at 2065–2066 cm^{-1} was detected in all model solutions examined except for the 1:1 model solution, and is due to free selenocyanate ion in DMF. For the model solutions prepared in DMSO (see Figure 11), the peak corresponding to free selenocyanate ion is observed at the same wavenumber position (as in DMF) at 2065–2066 cm^{-1} in all solutions scanned. However, in the 2080–2120 cm^{-1} region of the DMSO Cu^{2+}/$NCSe^-$ model solution IR spectra, there is a broad, relatively weak absorption peak which contain a minor contribution from a Cu/selenocyanate complex ion species. However a weak DMSO-solvent-related peak overlaps in the same area of the spectrum. Hence it was not possible to confirm this assignment unequivocally, which means the complex ion species was recorded in Table II as being not detected (nd) for the 1:1 mole ratio solution.

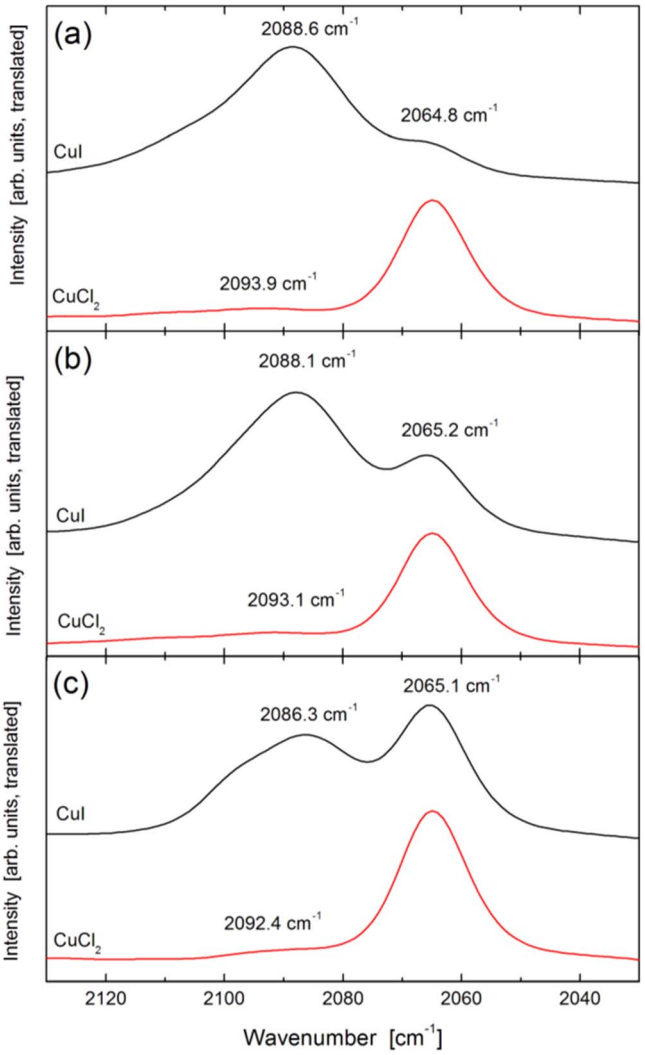

Figure 11. Transmission IR spectra of Cu(I) and Cu(II) pseudohalide complexes in the model solutions prepared with CuI and $CuCl_2$ salts at different mole ratios of Cu salt:pseudohalide salt in KSeCN salt/ DMSO model solution, where [CuI] or [$CuCl_2$] = 0.025 mol L^{-1} in each solution. (a) 1:1 CuI: $NCSe^-$ and 1:1 $CuCl_2$: $NCSe^-$ mole ratio solutions, (b) 1:2 CuI: $NCSe^-$ and 1:2 $CuCl_2$: $NCSe^-$ mole ratio solutions, (c) 1:4 CuI: $NCSe^-$ and 1:4 $CuCl_2$: $NCSe^-$ mole ratio solutions.

As stated earlier, the evidence for generation of a mixture of Cu(I) and Cu(II) selenocyanate complex ions in 1) the electrochemical cell during anodic dissolution in a SNIFTIRS experiment and 2) in the model solutions involving $CuCl_2$/KSeCN vs. CuI/KSeCN model solutions, cannot be as clearly demonstrated as it is when examining the Cu/thiocyanate solution data (see Figure 11a to 11c). The colors of the Cu(I) and Cu(II) selenocyanate model solutions are very similar, meaning that it is not possible to use the solution color to unequivocally identify the oxidation state of Cu in the cell solution during anodic dissolution in DMF or DMSO solutions of $NCSe^-$ ion. However it would not be unreasonable to speculate that both Cu(I) and Cu(II) species are present in such systems, as it is known from reported literature that redox chemistry also occurs when mixing Cu^{2+} ions with $NCSe^-$ ions in solution.[52]

XANES of Cu/$NCSe^-$ systems in DMSO (electrochemically generated and model solutions).—The XANES spectra for the electrochemically generated solutions and model solutions for the Cu/$NCSe^-$/DMSO system are shown in Figure 12. The 1:1 mole ratio ($CuCl_2$:KSeCN)

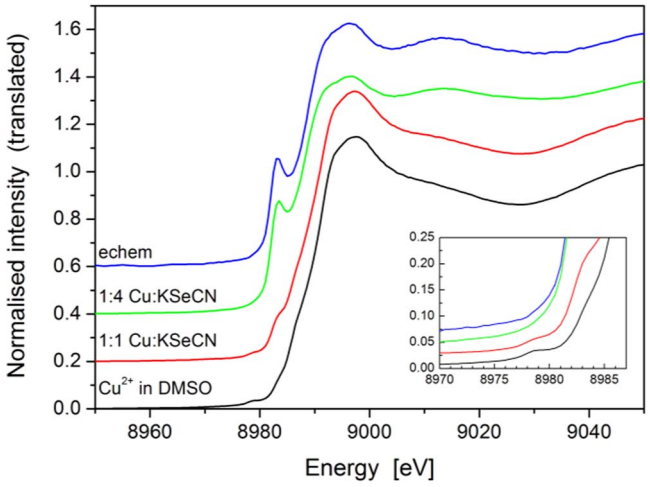

Figure 12. XANES scans of the model solutions prepared by adding Cu^{2+} and $NCSe^-$ in mole ratios of 1:1 and 1:4, and of the solution generated from the Cu/$NCSe^-$/DMSO electrochemical cell system (produced by polarizing the electrode at +400 mV for 2–3 hours). The "Cu^{2+} in DMSO" standard is also shown for comparison. The inset shows the pre-edge region. The spectra are normalized to a step height of 1 above the edge, and are subsequently offset for clarity.

model solution resembles the Cu/NCS^-/DMSO XANES (Figure 8), by having a pre-edge peak at 8979 eV and a shoulder at 8983 eV. The 1:4 mole ratio ($CuCl_2$:KSeCN) model solution and the electrochemically generated solution both exhibit a prominent peak on the edge at 8983 eV, and little to no pre-edge peak at 8979 eV. These features indicate that Cu in the 1:1 mole ratio model solution is mostly Cu^{2+}, while for the 1:4 model solution the electrochemically generated solution it is mostly Cu^+. As noted for the $CuCl_2$/KSCN model solution systems discussed earlier, there is a known redox reaction[52] between Cu^{2+} and $NCSe^-$ ions which results in a Cu(I) species being produced. XANES spectra in Figure 12 show that this becomes more dominant in the model solutions as the mole ratio of $CuCl_2$:KSeCN changes from 1:1 to 1:4. In the 1:1 mole ratio model solution, the feature at 8983 eV is minor indicating a relatively small amount of Cu(I) produced by the reaction so that the XANES spectrum more closely resembles a solution which is dominated by Cu(II) species. This is because there are equimolar amounts of $NCSe^-$ and Cu^{2+} in solution. As the mole ratio of $NCSe^-$ relative to Cu^{2+} increases, the peak at 8983 eV becomes more prominent, which indicates relatively more Cu(I) species are being produced in the model solutions as a result of the redox reaction between Cu^{2+} and $NCSe^-$. This provides strong evidence for the existence of mixed Cu(I)/Cu(II) –selenocyanate complex ion species in these electrochemical systems.

Discussion: effect of pseudohalide ion on the electrochemistry of the Cu/DMF/NCX^- and Cu/DMSO/NCX^- systems (X = O,S,Se).— The work described has shown that some commonalities and differences in electrochemical behavior occur across the series of pseudohalides examined. From SNIFTIRS and XANES data, it is clear that all Cu electrodes dissolve in the solutions of pseudohalide ions to produce Cu-pseudohalide complex ions in which the Cu(I) oxidation state features prominently. For the Cu/NCO^- electrochemical system, Cu(I) cyanate complexes are observed at very negative values of the applied potential. This has been ascribed to several factors as discussed previously, one of which is that there is a pre-existing passivation layer on the Cu surface consisting of adsorbed and solvated Cu(I) species. This behavior was also partially in accord with that discussed by Bron and Holze[12] in their reported SNIFTIRS study of cyanate and thiocyanate adsorption on Cu and Au electrodes, which reported that cyanate adsorbs on Cu electodes at more negative potentials relative to Au electrodes.

In contrast, the Cu/NCS^-/DMF or DMSO and the Cu/$NCSe^-$/DMF or DMSO electrochemical systems show spectroscopic and (cell) solution color evidence for formation of Cu(II) species in the IR spectroelectrochemical cell. This has been supported in part by the model solution data which are fortuitously complicated by the known redox reactions that occur between Cu(II) and NCS^- or $NCSe^-$ ions. These redox reactions lead to mixtures of both Cu(II) *and* Cu(I) species being present in the model solutions, something that also happens in the Cu/NCS^- and Cu/$NCSe^-$ electrochemical systems during the SNIFTIRS experiments. There is also evidence from SNIFTIRS spectra of deposition of solid films on the Cu electrode surface in the Cu/NCS^- and Cu/$NCSe^-$ electrochemical systems due to the low solubility of the solids produced in the thin layer. In contrast the Cu/NCO^- electrochemical systems show no detectable deposited solids in SNIFTIRS spectra.

Other differences in electrochemical behavior across the pseudohalide ion series relate to how each of the systems behave in DMSO and DMF with respect to CO_2 formation. For instance in DMF, both Cu/NCO^- and Cu/NCS^- electrochemical systems studied display evidence for formation of CO_2 during the SNIFTIRS experiment, whereas no evidence for CO_2 formation is observed for the Cu/$NCSe^-$ electrochemical system. CO_2 was not observed in any of the systems with DMSO as the solvent. This is reflective of DMF's stronger tendency to become electro-oxidized relative to DMSO.[53]

Conclusions

SNIFTIRS and XANES data have yielded interesting and novel information for identifying the Cu speciation in electrochemical systems where Cu electrodes are electrically polarized over a range of cathodic and anodic potentials in DMSO and DMF-based electrolyte media containing pseudohalide ions (NCO^-, NCS^- and $NCSe^-$). This fills a gap in the fundamental knowledge on the electrochemical behavior of such systems. In general, Cu(I) species complexed with pseudohalide ions were found to be present in all the electrochemical systems examined, which was reasoned to be a consequence of the presence of pre-existing Cu(I) species on the Cu electrode surface due to the reactivity of the metal. The presence of this film was believed to cause the appearance of $[Cu(NCO)_2]^-$ ions at very negative applied potentials. In the Cu/NCS^- and Cu/$NCSe^-$ electrochemical systems studied, Cu^{n+}/pseudohalide ion complexes were observed at less cathodic potentials relative to the Cu/NCO^- electrochemical systems, with IR and XANES evidence collectively indicating that the Cu^{n+}/thiocyanate or selenocyanate complex ions generated in SNIFTIRS experiments were actually a mixture of oxidation states of Cu(I) and Cu(II). The Cu/NCS^- and Cu/$NCSe^-$ electrochemical systems were also shown to form solid films of CuSCN and $K(SeCN)_3$ respectively when polarized at anodic potentials. IR transmission spectral data collected from model solutions prepared for all Cu/NCX^- systems studied provided convincing evidence to support the assignments of the electrogenerated complex ion species of Cu detected in SNIFTIRS experiments.

Acknowledgments

Portions of this work were undertaken on the X-ray Absorption Spectroscopy (XAS) Beamline at the Australian Synchrotron, Victoria, Australia. The authors are grateful for beamtime provided by the Australian Synchrotron as well as travel and accommodation funding granted by the New Zealand Synchrotron Group.

References

1. R. S. Goncalves and A. M. S. Lucho, *J. Braz. Chem. Soc.*, **11**, 486 (2000).
2. R. S. Vakhidov, *Russ. J. Electrochem.*, **30**, 1165 (1994).
3. B. Kratochvil and K. R. Betty, *J. Electrochem. Soc.*, **121**, 851 (1974).
4. V. Vojinovic, V. Komnenic, M. Pjescic, and S. Mentus, *J. Serb. Chem. Soc.*, **65**, 671 (2000).
5. C. Furlani, L. Sestili, A. Ciana, and F. Garbassi, *Electrochim. Acta*, **12**, 1393 (1967).

6. L. Sestili, C. Furlani, A. Ciana, and F. Garbassi, *Electrochim. Acta*, **15**, 225 (1970).
7. S. G. Biallozor and A. Lisowska, *Elektrokhimiya*, **15**, 634 (1979).
8. P. A. Kilmartin and G. A. Wright, *J. Chem. Soc. Faraday Trans.*, **91**, 4403 (1995).
9. G. A. Bowmaker, P. A. Kilmartin, and G. A. Wright, *J. Solid State Electrochem.*, **3**, 163 (1999).
10. G. A. Bowmaker and D. A. Rogers, *J. Chem. Soc., Dalton Trans.*, 1873 (1982).
11. P. A. Kilmartin and G. A. Wright, *Aust. J. Chem.*, **50**, 321 (1997).
12. M. Bron and R. Holze, *J. Electroanal. Chem.*, **385**, 105 (1995).
13. L. K. H. K. Alwis, M. R. Mucalo, and B. Ingham, *J. Electrochem. Soc.*, **160**, H803 (2013).
14. B. Bozzini, M. Kazemian Abyaneh, B. Busson, G. P. de Gaudenzi, L. Gregoratti, C. Humbert, M. Amati, C. Mele, and A. Tadjeddine, *J. Power Sources*, **231** (2013).
15. K. Brandt, E. Vogler, M. Parthenopoulos, and K. Wandelt, *J. Electroanal. Chem.*, **570**, 47 (2004).
16. J. G. Love, P. A. Brooksby, and A. J. McQuillan, *J. Electroanal. Chem.*, **464**, 93 (1999).
17. C. A. Melendres, G. A. Bowmaker, K. A. B. Lee, and B. Beden, *J. Electroanal. Chem.*, **449**, 215 (1998).
18. M. R. Mucalo and Q. Li, *J. Colloid Interface Sci.*, **269**, 370 (2004).
19. M. J. Smieja, M. D. Sampson, K. A. Grice, E. A. Benson, J. D. Froehlich, and C. P. Kubiak, *Inorg. Chem.*, **52**, 2484 (2013).
20. R. M. Souto, F. Ricci, L. Spyrkowicz, J. L. Rodriguez, and E. Pastor, *J. Phys. Chem. C*, **115**, 3671 (2011).
21. N. Xu, J. Lilly, D. R. Powell, and G. B. Richter-Addo, *Organometallics*, **31**, 827 (2012).
22. Y. Y. Yang, J. Ren, H.-X. Zhang, Z.-Y. Zhou, S.-G. Sun, and W.-B. Cai, *Langmuir*, **29**, 1709 (2013).
23. L. K. H. K. Alwis and M. Mucalo, *J. Electrochem. Soc.*, **161**, H738 (2014).
24. K. H. K. L. Alwis, B. Ingham, M. R. Mucalo, P. Kappen, and C. Glover, *RSC Advances*, **5**, 15709 (2015).
25. M. Newville, P. Livins, Y. Yacoby, J. J. Rehr, and E. A. Stern, *Phys. Rev. B: Condens. Matter*, **47**, 14126 (1993).
26. B. Ravel and M. Newville, *J. Synchrotron Radiat.*, **12**, 537 (2005).
27. D. Forster and D. M. L. Goodgame, *J. Chem. Soc.*, 262 (1965).
28. C. A. Melendres, G. A. Bowmaker, J. M. Leger, and B. Beden, *Nucl. Instrum. Methods Phys. Res., Sect. B*, **133**, 109 (1997).
29. A. Ray, G. M. Rosair, R. Rajeev, R. B. Sunoj, E. Rentschler, and S. Mitra, *Dalton Trans.*, 9510 (2009).
30. S. Ahrland, P. Blaeuenstein, B. Tagesson, and D. Tuhtar, *Acta Chem. Scand., Ser. A*, **A34**, 265 (1980).
31. J. L. Burmeister and T. P. O'Sullivan, *Inorg. Chim. Acta*, **3**, 479 (1969).
32. F. A. Cotton and G. Wilkinson, *Advanced Inorganic Chemistry: A Comprehensive Text*, pp. 799, Wiley, New York (1980).
33. J. Kohout, M. Hvastijova, and J. Gazo, *Coord. Chem. Rev.*, **27**, 141 (1978).
34. F. E. Huggins, G. P. Huffman, and J. D. Robertson, *J. Hazard. Mater.*, **74**, 1 (2000).
35. P. Frank, M. Benfatto, B. Hedman, and K. O. Hodgson, *Inorg. Chem.*, **51**, 2086 (2012).
36. J. S. McEwen, T. Anggara, W. F. Schneider, V. F. Kispersky, J. T. Miller, W. N. Delgass, and F. H. Ribeiro, *Catalysis Today*, **184**, 129 (2012).
37. L. S. Kau, D. J. Spira-solomon, J. E. Penner-Hahn, K. O. Hodgson, and E. I. Solomon, *J.A.C.S.*, **109**, 6433 (1987).
38. E. I. Solomon and C. B. Bell III, in *Physical Inorganic Chemistry: Principles, Methods, and Models*, A. Bakac Editor, p. 1, John Wiley & Sons, Hoboken NJ (2010).
39. D. Forster and D. M. L. Goodgame, *Inorg. Chem.*, **4**, 823 (1965).
40. J. Rannou and M. Chabanel, *Inorg. Chem.*, **24**, 2319 (1985).
41. L. M. Kul'berg and A. K. Gorlinskii, *Russ. J. Gen. Chem*, **9**, 1707 (1939).
42. J. H. Clark and C. W. Jones, *Inorg. Chim. Acta.*, **179**, 41 (1991).
43. M. Kabesova, J. Kohout, and J. Gazo, *Inorg. Chim. Acta*, **31**, L435 (1978).
44. S. K. Tobia, E. R. Souaya, and W. G. Hanna, *Polyhedron*, **4**, 425 (1985).
45. R. A. Bailey, L. S. Kozak, T. W. Michelsen, and W. N. Mills, *Coord. Chem. Rev.*, **6**, 407 (1971).
46. A. H. Norbury, in *Advances in Inorganic Chemistry and Radiochemistry*, H. J. Emeleus and A. G. Sharpe Editors, p. 231, Academic Press, Inc (London) Ltd., New York (1975).
47. A. Manceau and D. Gallup, *Environ. Sci. Technol.*, **31**, 968 (1997).
48. E. E. Aynsley, N. N. Greenwood, and M. J. Sprague, *J. Chem. Soc.*, 699 (1964).
49. F. Cataldo, *Polyhedron*, **19**, 681 (2000).
50. C. J. Burchell, P. Kilian, A. M. Z. Slawin, and J. D. Woollins, *Inorg. Chem.*, **45**, 710 (2006).
51. A. Solangi, A. M. Bond, I. Burgar, A. F. Hollenkamp, M. D. Horne, T. Ruther, and C. Zhao, *J. Phys. Chem. B*, **115**, 6843 (2011).
52. T. Krogulec, *Polish Journal of Chemistry*, **69**, 746 (1995).
53. H. Lund, in *Organic Electrochemistry*, H. Lund and O. Hammerich Editors, p. 265, Marcel Dekker, New York (1991).